EUROPEAN HEMATOLOGY ASSOCIATION
haematologica
Journal of the European Hematology Association

TIRAP p.R81C is a novel lymphoma risk variant which enhances cell proliferation via NF-κB mediated signaling in B-cells

by Regula Burkhard, Irene Keller, Miroslav Arambasic, Darius Juskevicius, Alexandar Tzankov, Pontus Lundberg, Rémy Bruggman, Stephan Dirnhofer, Ramin Radpour, and Urban Novak

Haematologica 2018 [Epub ahead of print]

Citation: Regula Burkhard, Irene Keller, Miroslav Arambasic, Darius Juskevicius, Alexandar Tzankov, Pontus Lundberg, Rémy Bruggman, Stephan Dirnhofer, Ramin Radpour, and Urban Novak. TIRAP p.R81C is a novel lymphoma risk variant which enhances cell proliferation via NF-κB mediated signaling in B-cells. Haematologica. 2018; 103:xxx
doi:10.3324/haematol.2018.201590

TIRAP p.R81C is a novel lymphoma risk variant which enhances cell proliferation via NF-κB mediated signaling in B-cells

Regula Burkhard[1,2,3], Irene Keller[4], Miroslav Arambasic[1,2,3], Darius Juskevicius[5], Alexandar Tzankov[5], Pontus Lundberg[6], Rémy Bruggmann[4], Stephan Dirnhofer[5], Ramin Radpour[1,7,*] and Urban Novak[1,3,*,+]

[1] Department of Medical Oncology, Inselspital, Bern University Hospital, University of Bern, Bern, Switzerland.

[2] Division of Experimental Pathology, Institute of Pathology, University of Bern, Bern, Switzerland.

[3] Department for BioMedical Research (DBMR), University of Bern, Bern, Switzerland.

[4] Interfaculty Bioinformatics Unit, Department for BioMedical Research, and Swiss Institute of Bioinformatics, Bern, Switzerland.

[5] Institute of Pathology and Medical Genetics, University of Basel, Basel, Switzerland.

[6] Department of Biomedicine, Experimental Hematology, University Hospital Basel and University of Basel, Basel, Switzerland.

[7] Tumor Immunology, Department for BioMedical Research (DBMR), University of Bern, Bern, Switzerland.

[*] Co-senior authors

[+] to whom correspondence should be addressed

Running title: *TIRAP*, a novel familial lymphoma risk gene

Correspondence:
Urban Novak, Department of Medical Oncology, Inselspital / Bern University Hospital, and University of Bern, CH-3010 Bern, Switzerland. E-mail: urban.novak@insel.ch, Tel: +41 31 632 41 14, Fax: +41 31 632 41 19.

Text word count:	4015
Abstract word count:	247
Number of figures:	7
Supplemental Data:	7 figures and 7 tables
Number of references:	50

Financial support: This work was supported by grants from the "Bernische Krebsliga", the "Werner und Hedy Berger-Janser Stiftung", the "Bernische Stiftung für klinische Krebsforschung", the "Stiftung für klinisch-experimentelle Tumorforschung", and a grant from the Inselspital/Bern University Hospital, all to U.N.

Conflict of interest: The authors declare no competing financial interest.

Abstract

Diffuse large B-cell lymphoma is the most common malignant lymphoma in adults. By gene-expression profiling, this lymphoma is divided in three cell-of-origin subtypes with distinct molecular and clinical features. Most lymphomas arise sporadically, yet familial clustering is known, suggesting a genetic contribution to disease risk. Familial lymphoma cases are a valuable tool to investigate risk genes. We studied a Swiss/Japanese family with two sisters affected by a primary mediastinal B-cell lymphoma and a non-germinal center diffuse large B-cell lymphoma not otherwise specified, respectively. The somatic landscape of both lymphomas was marked by alterations affecting multiple components of the JAK-STAT pathway. Consequently, this pathway was constitutively activated as evidenced by high pJAK2 as well as increased nuclear pSTAT3 and pSTAT6 in malignant cells. Potential lymphoma risk variants were identified by whole-exome sequencing of the germline DNA derived from siblings and unaffected family members. This analysis revealed a pathogenic variant in *TIRAP*, an upstream regulator of NF-κB, in both affected siblings and their mother. We observed increased B-cell proliferation in family members harboring the TIRAP p.R81C variant. B-cell proliferation correlated with *TIRAP* and NF-κB target gene expression, suggesting enhanced NF-κB pathway activity in TIRAP p.R81C individuals. *TIRAP* knockdown reduced B-cell survival and NF-κB target gene expression, particularly in individuals with TIRAP p.R81C. Functional studies revealed significantly increased NF-κB activity and resistance to stress-induced cell-death by TIRAP p.R81C. The identification of an inherited *TIRAP* variant provides evidence for a novel link between genetic alterations affecting the NF-κB pathway and lymphomagenesis.

Introduction

Diffuse large B-cell lymphoma (DLBCL) is the most common lymphoma in adults.[1] Its molecular subtypes, activated B-cell-like (ABC), germinal center B-cell-like (GCB) DLBCL, and primary mediastinal B-cell lymphoma (PMBL) arise from B-cells at distinct differentiation stages. [2,3] PMBL is clinically aggressive with bulky mediastinal masses. It accounts for up to 10% of DLBCLs, and preferentially occurs in young female patients.

Next-generation sequencing provided insights in genetic lesions of *de novo* DLBCL and its subtypes.[4–10] The genetic hallmarks of PBML are amplifications of the 9p24 locus containing *JAK2* and *PDL1*. Present in 70% of PMBL, this amplification is rare in other DLBCL subtypes.[11–13] Constitutive NF-κB pathway activity through various mechanisms is characteristic of PMBL and ABC-DLBCL.[14]

Until now, the knowledge on genetic risk factors for DLBCL/PMBLs remains obscure. Population-based studies reported an increased risk for DLBCL in relatives of individuals with DLBCL and genome-wide association studies identified several common single nucleotide variants associated with sporadic DLBCL.[15–18] Familial clustering provides evidence for Mendelian susceptibility. In very rare cases, familial aggregation is associated with hereditary cancer syndromes.[18] Outside those syndromes, a heritable basis for DLBCL is poorly understood. A germline variant in *MLL* described in a Finnish family is yet the only reported variant linked to familial PMBL.[19] Although familial lymphomas account for less than 5% of cases, these pedigrees are a valuable tool to identify risk genes that might also contribute to a better understanding of more frequent sporadic cases.

Here, we investigate a Swiss/Japanese family in which two out of three children were diagnosed with aggressive B-cell lymphomas arising in the mediastinum. Whole exome sequencing (WES) on the germline DNA of the affected siblings and healthy family members identified a variant in the TIR-domain-containing adaptor protein (TIRAP). TIRAP engages signals from TLR2 and TLR4 receptors and recruits MyD88 to the plasma membrane mediated through Toll/interleukin-1 receptor (TIR) domain interaction.[20] Downstream signaling includes activation of IL-1R-associated kinases (IRAK) ultimately culminating in the activation of the transcription factors NF-κB and AP-1. In this family, we identified an inherited TIRAP p.R81C variant in two affected siblings. This variant provided B-cells with increased proliferation and survival, through enhanced NF-κB activity. Functional studies revealed that TIRAP p.R81C enhanced NF-κB gene signature and reduced stress-triggered cell death. Collectively, we provide evidence that TIRAP p.R81C may act as a novel lymphoma risk variant and our data suggest that *TIRAP* should be integrated into the complex network of genes contributing to deregulated NF-κB signaling involved in lymphomagenesis.

Methods

Patients

Samples from patients, non-affected family members and healthy donors were collected with informed consent. This study was approved by the local ethical committee (KEK-BE116/11) and was conducted in accordance with the Declaration of Helsinki. The diagnosis of DLBCL/PMBL was according to the 2017 World Health Organization classification and pathological review by SD and AT confirmed the diagnosis.[1] Genomic DNA was extracted from peripheral blood mononuclear cells (PBMCs) using standard methods. Tumor DNA was isolated from formalin-fixed paraffin embedded tissues (FFPE) using phenol-chloroform. In FFPE samples, tumor cell-rich areas were identified on CD20 stained sections and separated from surrounding tissue by laser microdissection.

Whole-exome sequencing

The quality of extracted DNA was assessed by Bioanalyzer (Agilent) and a PCR fragment size-based assay developed at Fasteris (Geneva, Switzerland). Prior to library preparation with TruSeq DNA Sample Preparation Kit (Illumina), DNA samples were treated with PreCR Repair Mix (New England Biolabs). Exome capturing was performed using TruSeq Exome Enrichment Kit (Illumina) and samples were sequenced on an Illumina HiSeq2500 instrument with 100bp paired-end reads (Fasteris, sequencing performed between 2012 and 2014). As the FFPE lymphoma sample of sister 2 resulted in a low-yield library of poor quality, the library preparation was modified: after PreCR Repair mix treatment, DNA was split, and four libraries were prepared simultaneously using the Nextera Exome Enrichment Kit (Illumina). Before exome enrichment, libraries were pooled and sequencing was performed as described above. Both exome enrichment kits contained the same set of baits, resulting in identical exome coverage. WES data has been deposited at the European Nucleotide Archive (http://www.ebi.ac.uk/ena, accession number PRJEB15254). See supplemental Table 3 for exome data metrics.

Analysis of germline and somatic variants

Raw sequence read quality was assessed using FastQC. Reads were mapped to the human reference genome hg19 using Bowtie-2 v.2.2.1, and duplicated reads were removed by Picard-tools v.1.80. Germline variant calling was performed using the Genome Analysis Toolkit (GATK v.3.3.0) best practices workflow using Haplotype Caller and limiting the analysis to enriched targets ±100bp. We used GATK v.3.3.0 to recalibrate the variant quality and refine the genotypes using population (1000 Genomes Project, phase 1 data) and pedigree information. Variants in low complexity regions were removed.[21] Germline variants were prioritized as following: 1) good quality genotype in both sisters (Phred quality ≥20), 2) moder-

ate/high impact based on SnpEff v.3.2 prediction, 3) novel/known variant at frequency of less than 1% (not polymorphisms) according to the 1000 Genomes Database and the Exome Variant Server, and 4) the presence of at least one copy of the putatively harmful allele in both siblings. Only variants not present as homozygote in healthy family members were selected. Possible links between genes with germline variants and terms related to cancer and malignant lymphomas was assessed by Ariadne Genomics Pathway Studio v.9 (Elsevier). Alterations with a predicted link to the disease were annotated with PolyPhen-2, SIFT, MutationTaster and GERP++ effect prediction scores using dbNSFP v.2.1, and CADD scores v.1.1 from the CADD website. Pathway Studio was used to identify gene networks and canonical pathway enriched for genes containing putatively deleterious variants. The enrichment-scores were calculated using chi-square test comparing genes with putatively deleterious mutations to the proportion of background genes in the Gene Ontology group. An enrichment-score ≥3 corresponded to a significant link (*P<0.05*). See also supplemental methods.

Results

Clinical and histopathological characterization of the mediastinal B-cell lymphomas

The investigated Swiss/Japanese family encompasses two female siblings with lymphomas (Figure 1). The older sister 1 developed a PMBL at the age of 30 and died with primary progressive disease (Supplemental Table 1). At the age of 25, sister 2 was diagnosed with a stage IIA non-germinal center (GC) DLBCL, not otherwise specified (NOS) with a mediastinal mass and cervical lymphadenopathy. Chemo-immunotherapy achieved an ongoing remission. Smoldering myelomas IgGλ were detected in the father and his monozygotic twin at the age of 65 years. Other family members are currently healthy, and there are no other hematological malignancies in the extended family.

Both lymphomas lacked evidence of an Epstein-Barr virus infection (Supplemental Table 2), showed a clear cytoplasm and compartmentalizing sclerosis, and were CD20, CD30 and Ki-67 positive. However, the GC markers BCL6, CD10 and GCET1 were only expressed in the PMBL of sister 1, as was CD23 and BCL2. Despite the expression of CD30 and sclerosis, the clinical presentation, morphology and immunophenotype of the tumor in sister 2 were consistent with a non-GC DLBCL NOS.[1] Given its genetic (9p24 and 12q13 gains, *SOCS1* and *STAT6* mutations), and phenotypic characteristics (expression of CD30, overexpression of JAK2-STAT-cascade members), this lymphoma can retrospectively be considered to most probably represent a PMBL, and was initially designated as non-GC DLBCL NOS with features of PMBL.

Analysis of the coding genome of lymphomas

The somatic landscape of both lymphomas was analyzed by WES using the Illumina technology on DNA derived from laser-dissected FFPE tissue sections (Supplemental methods). Mutations were validated using Ion Proton sequencing, and their somatic origin was confirmed by the absence in matched normal DNA isolated from PBMCs. A total of 192 and 130 confirmed clonal protein altering mutations were identified in the lymphomas of sister 1 and 2, respectively (Supplemental Table 7). Most of those mutations were missense mutations, with a low number of nonsense and splice site variants (Figure 2A).

In addition, somatic copy number alterations (CNA) were analyzed by array comparative genomic hybridization (aCGH). While the tumor of sister 1 contained seven gains and two deletions, three gains were detected in the lymphoma of sister 2. Interestingly, 9p24 and 12q13 gains were present in both lymphomas (Figure 2B). FISH analyses revealed a trisomy at 8q24 (including *MYC)* in the lymphoma of sister 1, in line with the gain on chromosome 8 by aCGH (Figure 2B and 4B). Taken together, the analysis of CNA and somatic mutations reflected the known complex genetic landscape in those entities. The overall number of somatic lesions in the lymphoma of sister 1 was considerably higher (Figure 2C).

The JAK-STAT pathway has somatic mutations in multiple genes and is constitutively active

As mentioned above, aCGH revealed a 9p24 gain in both lymphomas (Figure 3A). The amplification of *JAK2*, a key target of the 9p24 gain, in both tumors was confirmed by FISH (Figure 3B). Moreover, a gain of 12q13 encompassing *STAT2* and *STAT6*, was detected in both lymphomas (Figure 3C). Besides CNA, we also identified somatic mutations in key genes of the JAK-STAT pathway. Each tumor harbored a private missense mutation within the DNA binding domain of STAT6 (Figure 3D). In addition, *SOCS1*, encoding a negative regulator of the JAK-STAT pathway, was mutated in the lymphoma of sister 1 (Figure 4A). Collectively, these somatic alterations caused constitutive activation of the JAK-STAT pathway as evidenced by high cytoplasmic expression of phosphorylated JAK2 (pJAK2) and increased nuclear pSTAT3 and pSTAT6 expression in most tumor cells (Figure 3E). In summary, despite distinct pathological and clinical features, these data revealed a shared aberrant activation of JAK-STAT signaling which is a known signature in PMBL.[22,23,10]

Genetic alterations related to the distinct clinical outcome

In contrast to ABC- and GCB-DLBCL, PMBLs have a favorable prognosis when responding to chemo-immunotherapy.[2] To investigate genetic lesions associated with the different clinical outcome, we focused on genes with a reported pathogenic role in lymphomas and/or genes which were mutated in more than 10% of DLBCLs.[4–10] Mutations in *B2M,* and *TP53*, *REL* and *MYC* gains as well as a *CIITA* break-apart were confined to the PMBL of sister 1

which died of primary progressive disease (Figure 4A, B). Although amplification of *PDL1* resulting from the 9p24 gain (Figure 4A) is a common feature of both lymphomas, PDL1 was only expressed on the malignant B-cells of sister 1 (Figure 4B).

The co-occurrence of genetic alterations involving genes related to immune-cell crosstalk in the lymphoma of sister 1 involving PDL1 expression, B2M p.M1R mutation and genomic alterations of *CIITA* are an interesting finding that suggests a combined role in escape from immune-surveillance.[24,25] In summary, we identified genetic lesions which may collectively contribute to the distinct clinical outcome. Of note, *TP53* mutations, *MYC* gains, *CIITA* translocation and expression of PDL1 on malignant B-cells, all solely present in the lymphoma of sister 1, have been associated with an inferior overall and progression free survival in DLBCL.[26–29] BCL2 expression, as observed in the lymphoma of sister 1, in the absence of a translocation (Supplemental Table 2) has a controversial prognostic role.[30]

Whole-exome sequencing identified lymphoma risk genes

The low age- and sex-adjusted incidence rate for sporadic DLBCL (0.1/100'000 cases in Switzerland[31]), and the occurrence of two siblings affected by mediastinal B-cell lymphomas suggested a genetic predisposition for lymphomagenesis in this family. Therefore, we performed WES on DNA from PBMCs of both sisters and all the other members of the core family (Figure 1). A total of 547 rare protein altering variants in 444 genes were identified out of 86-thousand screened variants in the germline DNA of each sister. After excluding variants which were present as homozygote in unaffected family members, 274 variants in 234 genes remained. To find a potential link between those 234 candidate genes and deregulated proliferation, we performed a comprehensive gene ontology and pathway enrichment analysis. The result indicated a significant link between 45 of these candidate genes with cancer and/or malignant lymphoma. To identify potential deleterious alterations, the pathogenicity of variants in those 45 cancer-related genes was examined by five different *in silico* algorithms. At the end, 15 variants in 15 candidate genes were predicted as deleterious by all algorithms and were considered for further analyses (Supplemental Figure 1A). Mutated genes were significantly enriched in processes like proliferation, lymphocyte activation and response to DNA damage, all pathways crucial for tumorigenesis (Supplemental figure 1B). Of note, *MLL* the currently only reported PMBL/DLBCL susceptibility gene was not found to harbor variants in this family.[19]

Interestingly, we identified *TIRAP* among those candidates. TIRAP is an adapter protein which engages signals from TLR2 and 4 and thereby activates the NF-κB pathway. Dysregulation of the NF-κB pathway is the oncogenic hallmark of ABC-DLBCL and PMBL.[14] Of note, in 420 primary DLBCLs, high *TIRAP* expression correlated with poor survival and

was significantly increased in high risk patients (data generated by SurvExpress[32], Supplemental Figure 2A). Besides, amplifications of 11q and 11q24 which also contain *TIRAP*, have been reported in about 20% of DLBCLs and PMBLs.[11,33,34] Somatic *TIRAP* mutations occurring in various cancers including DLBCL are listed in COSMIC and genomic sequencing studies on several hundred DLBCLs revealed somatic alterations in *TIRAP* in roughly 0.5% of cases.[34,35] However, the role of TIRAP in tumorigenesis has so far not been investigated. Hence, we functionally investigate if the identified *TIRAP* variant in this family contributes to lymphomagenesis.

TIRAP p.R81C variant is a potential novel risk factor for lymphomas

WES revealed a heterozygous variant within the coding exon 5 of *TIRAP* (c.241C>T) in both sisters and their Japanese mother. The variant was absent in other unaffected family members (Figure 5A). This variant resulted in a substitution of the arginine at amino acid residue 81 to a cysteine (p.R81C) which is highly conserved among species and located in close proximity to the functional TIR domain (Supplemental Figure 2B, C). The TIRAP p.R81C variant was predicted to be deleterious by five out of five applied algorithms (Supplemental Figure 2D), has a dbSNP identifier (rs138228187) and is reported in COSMIC. It has a global minor allele frequency of 0.00006 and 0.0006 in ExAC and 1000 Genomes, respectively and 0.0005 in the Japanese population, and is therefore not a polymorphism.[36,37] Sanger sequencing of cDNA derived from fresh PBMCs of the family members confirmed the TIRAP p.R81C status and expression of the variant allele in sister 2 and her mother (Figure 5A and Supplemental Figure 3). Of note, the p.R81C variant was also identified in the lymphomas of both siblings (data not shown).

To investigate the functional consequence of TIRAP p.R81C, we assessed the expression of pIRAK1 and total IRAK4, two downstream kinases and activators of the NF-κB signaling pathway. For IRAK4, our analysis was confined to the total protein, as an antibody to reliably determine its phosphorylated form on FFPE tissue was not available. GC B-cells of healthy controls showed little to no pIRAK1 and IRAK4 expression whereas p.R81C TIRAP carrying malignant B-cells of both sisters were clearly positive for these markers (Figure 5B, C). This suggests that the TIRAP downstream signaling is predominantly active in malignant B-cells with the p.R81C mutation. The relevance of this pathway is underlined by the analysis of 36 primary ABC-DLBCLs which revealed that 63% and 17% expressed pIRAK1 and IRAK4, respectively (Figure 5C). GCB-DLBCLs however, generally lacked the expression of both kinases.

To assess TIRAP/NF-κB pathway activity in non-malignant cells, we determined the gene expression of *TIRAP* as well as genes involved in cell proliferation and survival, among them

several targets of NF-κB in PBMCs of living family members. Unsupervised hierarchical clustering analysis revealed two clusters, separating TIRAP p.R81C and wild-type samples based on the expression signature of selected genes (Figure 5D). PBMCs carrying the TIRAP p.R81C mutation expressed higher levels of *TIRAP* as well as genes involved in cell survival, cell cycle and proliferation. Contrarily, *TIRAP* wild-type PBMCs showed higher expression of *CASP9* which is implicated in intrinsic apoptosis.

Next, we studied the impact of TIRAP p.R81C on primary B-cells. An increase of proliferating B-cells as determined by Ki-67 was observed in TIRAP p.R81C compared to TIRAP wild-type family members (Figure 5E). This was a surprising finding since circulating B-cells are generally quiescent[38,39] which we observed in age- and sex-matched healthy individuals as well as TIRAP wild-type family members. Sanger sequencing confirmed the absence of TIRAP p.R81C variant in healthy donors (Supplemental Figure 3). Activation of TLR through lipopolysaccharide (LPS) further enhanced B-cell proliferation, preferentially in TIRAP p.R81C individuals (Figure 5E). The higher level of assessed B-cell proliferation in TIRAP p.R81C cases was positively correlated with the increased gene expression levels of *TIRAP* as well as *BCL2L1* and *NFKB1* as main regulators of NF-κB signaling in PBMCs of all family members (Figure 5F). Collectively, our data indicate a potential role of p.R81C variant in activating NF-κB leading to enhanced B-cell proliferation and survival.

NF-κB signaling mediated by TIRAP is important for B-cell survival

To study the effect of TIRAP on cell survival, we performed a siRNA-mediated knockdown of endogenous *TIRAP* in PBMCs isolated from available family members. Overall, *TIRAP* knockdown efficiency was 60% at the mRNA level (Supplemental Figure 4A). *TIRAP* knockdown significantly diminished the number of living B-cells (Figure 6A, B). This effect was independent of the p.R81C, indicating that TIRAP is an important determinant for B-cells survival. Besides, we profiled the expression of genes important for cell survival and proliferation including NF-κB targets genes (Figure 6C). Silencing *TIRAP* strongly reduced the expression of the NF-κB target genes (*NFKB1*, *IL6* and *MYC*) in PBMCs, indicating that both wild-type and p.R81C TIRAP, mediate signal through the NF-κB pathway (Figure 6D and Supplemental figure 4). However, down-regulation of NF-κB target genes was more pronounced in TIRAP p.R81C PBMCs suggesting that these cells particularly rely on the NF-κB pathway (Figure 6E and Supplemental Figure 4). Consistent with the reduced B-cell survival, *CASP9* expression increased following *TIRAP* silencing in PBMCs with a higher extend in p.R81C mutated cells (Figure 6D, E). Interestingly, NF-κB signature was further reduced following stimulation with LPS (Supplemental Figure 5), supporting that TIRAP transduces signals from TLR4.[20]

TIRAP p.R81C drives NF-κB pathway activity and reduces stress-induced cell death

To evaluate the functional consequence of TIRAP p.R81C, 293T cells were transfected with bidirectional plasmids encoding for EGFP and TIRAP p.R81C, TIRAP WT or empty vector (control), respectively. Under homeostatic conditions, we did not observed changes in cell viability 24 hours post transfection (Supplemental figure 6). However, gene-expression analysis on GFP-positive transfected cells revealed increased expression of the NF-κB target genes *NFKB1*, *BCL2L1*, *CDKN2A* and *MYC* by TIRAP p.R81C compared to wild-type (Figure 7A). Thus, we tested whether these transcriptional changes could affect cell viability upon stress-induced challenge. Therefore, sorted GFP-positive cells were cultured in minimal starving media for 48 hours. Surprisingly, cell viability was significantly reduced in control or TIRAP WT transfected cells (Figure 7B). Remarkably, our data indicate that TIRAP p.R81C variant is an upstream activator of NF-κB which leads to a better cell survival/proliferation via enhanced NF-κB activity and decreased stress-induce cell death.

Discussion

The etiology of DLBCL is poorly understood. Familial clustering of lymphoma is reported to increase disease risk, indicating a role for genetic factors.[15,16] Although familial lymphoma cases are rare, studying such pedigrees might identify disease-causing variations and lead to a better understanding of lymphomagenesis. A Finnish family with three siblings affected by PMBL and a cousin with extranodal DLBCL has been described.[19] These lymphomas segregate with the p.H1845N mutation in MLL. The role of this variant in lymphomagenesis has not been corroborated by functional studies, and it is to the best of our knowledge, currently the only described DLBCL/PMBL predisposing mutation.

Here, we studied a Swiss/Japanese family with two sisters affected by B-cell lymphomas in the mediastinum. Although at initial diagnosis their lymphomas were considered as distinct DLBCL subtypes according to the current WHO classification,[1] the characterization of the somatic lesions by WES and aCGH revealed noticeable molecular similarities. Their somatic landscape is marked by multiple alterations affecting important players of the JAK-STAT signaling cascade which collectively lead to constitutive pathway activity, known to be crucially implicated in lymphomagenesis.[14] Shared gains of 9p24/*JAK2* and 12q13 (*STAT2* and *STAT6*) were detected by aCGH. Furthermore, we identified missense hotspot mutations in *STAT6* in both lymphomas (p.N417 and p.D417). A significant enrichment of *STAT6* mutations in PMBL has been described, with mutations being present in more than 30% of cases.[9,22] 9p24/*JAK2* gains are also recurrent genetic alterations in PMBL, but not strictly confined to this subtype.[13,40]

Constitutive activation of the NF-κB pathway is a hallmark of both ABC-DLBCL and PMBL and promotes survival of malignant cells. Somatic oncogenic mutations in components of the B-cell receptor signaling pathways including *CD79A/B* and *CARD11* activate NF-κB.[14] Gain-of-function mutations in *MYD88* have been described in 29% of ABC-DLBCLs.[14] Moreover, *TNFAIP3* which negatively regulates the NF-κB pathway is somatically inactivated in one third of ABC-DLBCLs and PMBLs.[14] Interestingly, germline mutation in *TNFAIP3* and *CARD11* have been described in lymphomas complicating primary Sjögren's syndrome and congenital B-cell lymphocytosis, respectively.[41,42] We searched for possible risk alleles associated with the lymphomas in the family investigated by WES, and discovered germline variants in *TIRAP* and *IL1R1* (detailed data on *IL1R1* not shown). The latter was not among the final candidate genes, as the homozygous mutation was present in all family members. Nevertheless, the presence of germline variants in two upstream regulators of NF-κB in a PMBL family is an interesting finding that supports the importance of the pathway in lymphomagenesis. Of note, our data support the cooperation between rare germline variants and constitutive pathway activation in malignant lymphomas.[43]

The predicted damaging effect of TIRAP p.R81C variant occurred at a highly conserved amino acid in close proximity to the functional TIR domain that is stabilized by two internal disulfide bonds.[44,45] Therefore, the substitution of an arginine by a cysteine might have implications on the TIRAP protein interaction with downstream signaling proteins. Of note, an arginine to cysteine mutation in MYD88, another adapter molecule involved in NF-κB signaling, diminished its interaction with TIRAP.[46]

In mice, deletion of *Tirap* reduced B-cell proliferation in response to TLR4 signaling.[20] Accordingly, we observed a direct correlation between B-cell proliferation and *TIRAP* expression. In this family, a high expression of *TIRAP* correlated with the p.R81C genotype. In 420 primary DLBLC cases, high *TIRAP* levels correlated with a poor survival and were significantly increased in high risk DLBCLs.[32,47] Furthermore, we linked the enhanced proliferation of TIRAP p.R81C B-cells with an increased expression of NF-κB target genes and genes involved in cell survival and proliferation in PBMCs. In this context, it is important to stress that we determined the lymphocytes to account for more than 65% of cells in the analyzed PMBC samples. Additionally, *TIRAP* knockdown was paralleled by a significant decrease in the gene expression signature of the NF-κB pathway, particularly in PBMCs carrying the p.R81C variant. Contrarily, overexpression of TIRAP p.R81C increased NF-κB gene signature *in vitro*. Moreover, TIRAP p.R81C expressing cells showed enhanced resistance to stress-induced apoptosis, indicating that TIRAP p.R81C provides a survival advantage under those conditions.

Our data link TIRAP p.R81C variant/expression with increased B-cell proliferation as well as survival, and thus add TIRAP to the existing network of lymphoma risk genes that are associated with deregulated NF-κB signaling such as *TNFAIP3*, *CD79A*/B, *MYD88* and *CARD11*. Interestingly, all these genes were unmutated in the lymphomas of both sisters. Similar to patients expressing the oncogenic p.L265P MYD88 variant, patients with aberrant TIRAP signaling might profit from IRAK4-selective kinase inhibitors.[48]

DLBCL is a polygenic disease with a complex pathogenesis. Therefore, additional alterations are required for the full malignant transformation of B-cells. Interestingly, all investigated family members were found to have a homozygous germline loss of *GSTT1*, a reported risk factor for lymphomas (Supplemental Figure 7).[18] One can hypothesize that the interplay of the germline TIRAP p.R81C variant and *GSTT1* loss coupled with additional genomic changes culminated in B-cell transformation in the investigated family. The identification of TIRAP p.R81C variant in a family with mixed ethnical background along with the demonstration of distinct targets of recurrent mutations in Chinese DLBCLs[49], might be an important additional aspect.

Overall, our findings revealed TIRAP p.R81C as a potential lymphoma risk variant in a family of mixed ethnical background. Through our analysis, we complement the existing view on the different players of the NF-κB pathway crucially involved in DLBCL.

Acknowledgements

The authors would like to thank Magne Osteras and his team at Fasteris (Geneva, Switzerland) for their excellent technical assistance. The probe for the *TNFAIP3* FISH analysis was a gift from Laura Pasqualucci and Riccardo Dalla-Favera (Institute for Cancer Genetics, Columbia University, New York, USA). The determination of *CIITA* rearrangement by FISH was kindly performed by Laurence de Leval (Institute of Pathology, Centre Hospitalier Universitaire Vaudois, Lausanne, Switzerland). We thank Lukas Mager, Deborah Krauer, Mario P. Tschan, Emilly Auma, Adrian F. Ochsenbein, Radek Skoda, Federico Santoni, André Schaller, and Outi Kilpivaara for helpful discussions and critical comments.

Author contributions

RB and UN designed the study; RB, MA, RR and DJ performed experiments; RB, IK, MA, RR, DJ, PL, RB, AT and SD analyzed the data. RB and UN wrote manuscript, and all authors contributed to and agreed to the final version of the manuscript.

References

1. Swerdlow SH, World Health Organization, International Agency for Research on Cancer, editors. WHO classification of tumours of haematopoietic and lymphoid tissues. Revised 4th edition. Lyon: International Agency for Research on Cancer; 2017.

2. Rosenwald A, Wright G, Leroy K, et al. Molecular diagnosis of primary mediastinal B cell lymphoma identifies a clinically favorable subgroup of diffuse large B cell lymphoma related to Hodgkin lymphoma. J Exp Med. 2003;198(6):851–862.

3. Savage KJ, Monti S, Kutok JL, et al. The molecular signature of mediastinal large B-cell lymphoma differs from that of other diffuse large B-cell lymphomas and shares features with classical Hodgkin lymphoma. Blood. 2003;102(12):3871–3879.

4. Pasqualucci L, Trifonov V, Fabbri G, et al. Analysis of the coding genome of diffuse large B-cell lymphoma. Nat Genet. 2011;43(9):830–837.

5. Morin RD, Mendez-Lago M, Mungall AJ, et al. Frequent mutation of histone-modifying genes in non-Hodgkin lymphoma. Nature. 2011;476(7360):298–303.

6. Morin RD, Mungall K, Pleasance E, et al. Mutational and structural analysis of diffuse large B-cell lymphoma using whole-genome sequencing. Blood. 2013;122(7):1256–1265.

7. Lohr JG, Stojanov P, Lawrence MS, et al. Discovery and prioritization of somatic mutations in diffuse large B-cell lymphoma (DLBCL) by whole-exome sequencing. Proc Natl Acad Sci U S A. 2012;109(10):3879–3884.

8. Zhang J, Grubor V, Love CL, et al. Genetic heterogeneity of diffuse large B-cell lymphoma. Proc Natl Acad Sci. 2013;110(4):1398–1403.

9. Dubois S, Viailly P-J, Mareschal S, et al. Next-Generation Sequencing in Diffuse Large B-Cell Lymphoma Highlights Molecular Divergence and Therapeutic Opportunities: a LYSA Study. Clin Cancer Res. 2016;22(12):2919–2928.

10. Gunawardana J, Chan FC, Telenius A, et al. Recurrent somatic mutations of PTPN1 in primary mediastinal B cell lymphoma and Hodgkin lymphoma. Nat Genet. 2014;46(4):329–335.

11. Wessendorf S, Barth TFE, Viardot A, et al. Further delineation of chromosomal consensus regions in primary mediastinal B-cell lymphomas: an analysis of 37 tumor samples using high-resolution genomic profiling (array-CGH). Leukemia. 2007;21(12):2463–2469.

12. Joos S, Otaño-Joos MI, Ziegler S, et al. Primary mediastinal (thymic) B-cell lymphoma is characterized by gains of chromosomal material including 9p and amplification of the REL gene. Blood. 1996;87(4):1571–1578.

13. Lenz G, Wright GW, Emre NCT, et al. Molecular subtypes of diffuse large B-cell lymphoma arise by distinct genetic pathways. Proc Natl Acad Sci U S A. 2008;105(36):13520–13525.

14. Pasqualucci L, Dalla-Favera R. Genetics of diffuse large B cell lymphoma. Blood. 2018;131(21):2307–2319.

15. Altieri A, Bermejo JL, Hemminki K. Familial risk for non-Hodgkin lymphoma and other lymphoproliferative malignancies by histopathologic subtype: the Swedish Family-Cancer Database. Blood. 2005;106(2):668–672.

16. Goldin LR, Björkholm M, Kristinsson SY, Turesson I, Landgren O. Highly increased familial risks for specific lymphoma subtypes. Br J Haematol. 2009;146(1):91–94.

17. Cerhan JR, Berndt SI, Vijai J, et al. Genome-wide association study identifies multiple susceptibility loci for diffuse large B cell lymphoma. Nat Genet. 2014;46(11):1233–1238.

18. Skibola CF, Curry JD, Nieters A. Genetic Susceptibility to Lymphoma. Haematologica. 2007;92(7):960.

19. Saarinen S, Kaasinen E, Karjalainen-Lindsberg M-L, et al. Primary mediastinal large B-cell lymphoma segregating in a family: exome sequencing identifies MLL as a candidate predisposition gene. Blood. 2013;121(17):3428–3430.

20. Horng T, Barton GM, Medzhitov R. TIRAP: an adapter molecule in the Toll signaling pathway. Nat Immunol. 2001;2(9):835–841.

21. Li H. Toward better understanding of artifacts in variant calling from high-coverage samples. Bioinformatics. 2014;30(20):2843–2851.

22. Ritz O, Guiter C, Castellano F, et al. Recurrent mutations of the STAT6 DNA binding domain in primary mediastinal B-cell lymphoma. Blood. 2009;114(6):1236–1242.

23. Green MR, Monti S, Rodig SJ, et al. Integrative analysis reveals selective 9p24.1 amplification, increased PD-1 ligand expression, and further induction via JAK2 in nodular sclerosing Hodgkin lymphoma and primary mediastinal large B-cell lymphoma. Blood. 2010;116(17):3268–3277.

24. Mottok A, Woolcock B, Chan FC, et al. Genomic Alterations in CIITA Are Frequent in Primary Mediastinal Large B Cell Lymphoma and Are Associated with Diminished MHC Class II Expression. Cell Rep. 2015;13(7):1418–1431.

25. Challa-Malladi M, Lieu YK, Califano O, et al. Combined Genetic Inactivation of Beta2-Microglobulin and CD58 Reveals Frequent Escape from Immune Recognition in Diffuse Large B-cell Lymphoma. Cancer Cell. 2011;20(6):728–740.

26. Xu-Monette ZY, Wu L, Visco C, et al. Mutational profile and prognostic significance of TP53 in diffuse large B-cell lymphoma patients treated with R-CHOP: report from an International DLBCL Rituximab-CHOP Consortium Program Study. Blood. 2012;120(19):3986–3996.

27. Valera A, López-Guillermo A, Cardesa-Salzmann T, et al. MYC protein expression and genetic alterations have prognostic impact in patients with diffuse large B-cell lymphoma treated with immunochemotherapy. Haematologica. 2013;98(10):1554–1562.

28. Steidl C, Shah SP, Woolcock BW, et al. MHC class II transactivator CIITA is a recurrent gene fusion partner in lymphoid cancers. Nature. 2011;471(7338):377–381.

29. Kiyasu J, Miyoshi H, Hirata A, et al. Expression of programmed cell death ligand 1 is associated with poor overall survival in patients with diffuse large B-cell lymphoma. Blood. 2015;126(19):2193–2201.

30. Visco C, Tzankov A, Xu-Monette ZY, et al. Patients with diffuse large B-cell lymphoma of germinal center origin with BCL2 translocations have poor outcome, irrespective of MYC status: a report from an International DLBCL rituximab-CHOP Consortium Program Study. Haematologica. 2013;98(2):255–263.

31. Cancer data extracted from the Swiss national dataset managed by the Fondation National Institute for Cancer Epidemiology and Registration (NICER). Available from: http://www.nicer.org/. Accessed on February 2015. http://www.nicer.org/de/ (accessed September 15, 2016).

32. Lenz G, Wright G, Dave SS, et al. Stromal gene signatures in large-B-cell lymphomas. N Engl J Med. 2008;359(22):2313–2323.

33. Bonetti P, Testoni M, Scandurra M, et al. Deregulation of ETS1 and FLI1 contributes to the pathogenesis of diffuse large B-cell lymphoma. Blood. 2013;122(13):2233–2241.

34. Chapuy B, Stewart C, Dunford AJ, et al. Molecular subtypes of diffuse large B cell lymphoma are associated with distinct pathogenic mechanisms and outcomes. Nat Med. 2018;24(5):679–690.

35. Schmitz R, Wright GW, Huang DW, et al. Genetics and Pathogenesis of Diffuse Large B-Cell Lymphoma. N Engl J Med. 2018;378(15):1396–1407.

36. Richards S, Aziz N, Bale S, et al. Standards and Guidelines for the Interpretation of Sequence Variants: A Joint Consensus Recommendation of the American College of Medical Genetics and Genomics and the Association for Molecular Pathology. Genet Med. 2015;17(5):405–424.

37. Higasa K, Miyake N, Yoshimura J, et al. Human genetic variation database, a reference database of genetic variations in the Japanese population. J Hum Genet. 2016;61(6):547–553.

38. Caraux A, Klein B, Paiva B, et al. Circulating human B and plasma cells. Age-associated changes in counts and detailed characterization of circulating normal CD138− and CD138+ plasma cells. Haematologica. 2010;95(6):1016–1020.

39. Chong Y, Ikematsu H, Yamaji K, et al. CD27(+) (memory) B cell decrease and apoptosis-resistant CD27(-) (naive) B cell increase in aged humans: implications for age-related peripheral B cell developmental disturbances. Int Immunol. 2005;17(4):383–390.

40. Meier C, Hoeller S, Bourgau C, et al. Recurrent numerical aberrations of JAK2 and deregulation of the JAK2-STAT cascade in lymphomas. Mod Pathol. 2009;22(3):476–487.

41. Nocturne G, Boudaoud S, Miceli-Richard C, et al. Germline and somatic genetic variations of TNFAIP3 in lymphoma complicating primary Sjögren's syndrome. Blood. 2013;122(25):4068–4076.

42. Snow AL, Xiao W, Stinson JR, et al. Congenital B cell lymphocytosis explained by novel germline CARD11 mutations. J Exp Med. 2012;209(12):2247–2261.

43. Yang Y, Schmitz R, Mitala J, et al. Essential role of the linear ubiquitin chain assembly complex in lymphoma revealed by rare germline polymorphisms. Cancer Discov. 2014;4(4):480–493.

44. Valkov E, Stamp A, DiMaio F, et al. Crystal structure of Toll-like receptor adaptor MAL/TIRAP reveals the molecular basis for signal transduction and disease protection. Proc Natl Acad Sci. 2011;108(36):14879–14884.

45. Lin Z, Lu J, Zhou W, Shen Y. Structural Insights into TIR Domain Specificity of the Bridging Adaptor Mal in TLR4 Signaling. PloS One. 2012;7(4):e34202.

46. Bernuth H von, Picard C, Jin Z, et al. Pyogenic Bacterial Infections in Humans with MyD88 Deficiency. Science. 2008;321(5889):691–696.

47. Aguirre-Gamboa R, Gomez-Rueda H, Martínez-Ledesma E, et al. SurvExpress: an online biomarker validation tool and database for cancer gene expression data using survival analysis. PloS One. 2013;8(9):e74250.

48. Kelly PN, Romero DL, Yang Y, et al. Selective interleukin-1 receptor–associated kinase 4 inhibitors for the treatment of autoimmune disorders and lymphoid malignancy. J Exp Med. 2015;212(13):2189–2201.

49. Miranda NFCC de, Georgiou K, Chen L, et al. Exome sequencing reveals novel mutation targets in diffuse large B-cell lymphomas derived from Chinese patients. Blood. 2014;124(16):2544–2553.

50. Juilland M, Gonzalez M, Erdmann T, et al. CARMA1- and MyD88-dependent activation of Jun/ATF-type AP-1 complexes is a hallmark of ABC diffuse large B-cell lymphomas. Blood. 2016;127(14):1780–1789.

Figure legends

Figure 1. Mediastinal B-cell lymphomas arising in two female siblings. Pedigree of the studied Swiss/Japanese family. Circles and squares represent female and male family members, respectively. Open symbols indicate unaffected persons; closed symbols represent the two siblings affected by primary mediastinal B-cell lymphoma (PBML) and mediastinal non-germinal center (GC) diffuse large B-cell lymphoma (DLBCL), not otherwise specified (NOS), respectively. The deceased individual (sister 1) is marked by a slash through the symbol. The year of diagnosis is shown in brackets and the year of birth is denoted by a *. Both lymphomas were classified according to the World Health Organization classification from 2017.[1]

Figure 2. Overall load of numerical and structural genomic alterations in the lymphomas of both siblings. (A) Number of all validated (by IonProton sequencing) non-silent somatic clonal mutations identified through Whole-exome sequencing in the two tumors. (B) Chromosomal gains and losses detected in the two lymphomas by array comparative genomic hybridization (aCGH). In the aCGH profiles, the normalized log2 rations are plotted based on their chromosome position, with vertical bars separating the chromosomes. Regions with losses and gains are represented by decreased and increased log2 ratios, respectively. Genomic changes are marked in red (gain) and green (loss). Copy number (CN) alterations which are present in both tumors are underlined. (C) Combined load of somatic non-silent mutations as well as CN gains and losses identified in the two investigated lymphomas.

Figure 3. The JAK-STAT pathway has somatic mutations in multiple genes and is constitutively active. (A) aCGH probe view of the 9p24 gain. A duplication of the *JAK2* locus was detected in both samples, shown as an increase of the average log2 ratio above zero (bold line). Shaded area indicated the extent of a copy number aberration. (B) FISH signals with BAC probes for the 5' and 3' regions of *JAK2*. Arrows indicate examples of cells with multiple FISH signals. Note green autofluorescent sclerosing bundles in the background. Scale bars: 10µm. (C) aCGH probe view of gains in 12p13 region, which among other genes also affect *STAT2* and *STAT6* as indicated by arrows. (D) Top: Schematic representation of the human *STAT6* gene locus with open and closed boxes indicating noncoding and coding exons, respectively. Below: confirmed somatic missense mutations located within the DNA binding domain of STAT6. Protein domain annotation according to Pfam. (E) The expression of phosphorylated (p) pJAK2, pSTAT3 and pSTAT6 in the two lymphomas was assessed by IHC. Scale bars: 10µm.

Figure 4. Genetic alterations related to the different clinical outcome. (A) Comparison of the somatic landscape in the two lymphomas implementing the lesions identified by whole-exome sequencing, aGCH and FISH. Only alterations in genes which are present in more than 10% of DLBCL cases and/or with a pathogenic significance in lymphoid malignancies were considered for this comparison.[4–10] Mutations (M), copy number alterations (CN) and translocations (Tx) are sorted according to whether they were found to be mutated in both tumors or restricted to one lymphoma only. Numbers indicate the total amount of identified somatic mutations. In red, genes which have been associated with worse clinical outcome.[9,26–29] (B) Left: Representative FISH signal patterns using *MYC* and *CIITA* break apart assay in the PMBL of sister 1. Arrows indicate examples of cells with *MYC* (multiple FISH signals) gains and *CIITA* break apart (split red and green FISH signals), respectively. Scale bars: 10µm. Right: IHC analysis of PDL1 protein expression in the lymphoma of sister 1. Scale bar: 50µm.

Figure 5. TIRAP p.R81C a potential novel familial lymphoma risk variant. (A) Top: Schematic representation of the human *TIRAP* gene locus with open and closed boxes indicating noncoding and coding exons, respectively. Below: whole exome sequencing data for the affected region of the *TIRAP* exon 5 visualized in integrative genomic viewer demonstrating a heterozygous variant in both sisters and their mother, whereas homozygous wild-type sequence was observed in the remaining family members. Sanger sequence data of complementary (c) DNA isolated from fresh PBMCs showing the same variant. Of note, no cDNA was available for sister 1 (deceased). (B) IRAK1 phosphorylation (p) and IRAK4 expression was assessed by IHC in the two lymphomas as well as lymphoid tissue of (un-matched) healthy controls. Scale bars: 50µm. (C) Representation of the percentage of cells expressing pIRAK1 and total IRAK4 in samples described in (B) as well as 36 ABC-DLBCLs and 32 GCB-DLBCLs. The primary samples have been described previously.[50] (D) Heatmap showing hierarchical clustering of mRNA levels of genes involved in NF-κB pathway, cell survival and proliferation in PBMCs of mother (M), sister 2 (S2), brother (B) and father (F). The hierarchical cluster analysis (Euclidean's method) reveals two major clusters representing TIRAP p.R81C mutated and wild-type (WT) individuals. Bar chart showing the log2 fold difference in gene expression in TIRAP p.R81C versus WT family members. (E) PBMCs isolated from family members and age- and sex-matched healthy donors (HD) were cultured in the presence (+) or absence (-) of 10ng/ml lipopolysaccharide (LPS) for 12h. Ki-67 was measured by flow cytometry on $CD20^+$ B-cells. (F) Linear correlation (Pearson correlation) between Ki-67+ B-cells and *BCL2L1* (left), *NFKB1* (right) or *TIRAP* (below) expression in PBMCs as measured by flow cytometry and quantitative PCR (normalized to *ACTb*), respectively.

Figure 6. **NF-κB signaling mediated by TIRAP is important for B cell survival.** (A) PBMCs were isolated from family members and transfected with control (CTRL) or *TIRAP*-directed siRNA. Twenty-four hours following transfection, cell viability of $CD20^+$ B-cells was assessed by Annexin V/DAPI staining and flow cytometry analysis. A representative flow cytometry dot plot and quantification of living B-cell are shown in (A) and (B), respectively. Statistics: Student t test. *, *P<0.05*. (C) Heatmap showing hierarchical clustering of mRNA levels of genes involved in NF-κB pathway, cell survival and proliferation in PBMCs of mother (M), sister 2 (S2), brother (B) and father (F) treated as described in (A). Data were clustered using standard Euclidean's method based on the average linkage. (D) Bar chart showing the relative expression levels of *NFKB1*, *CASP9*, *IL6* and *MYC* genes normalized to *ACTb* in family members with wild-type (brother and father) and p.R81C (sister 2 and mother) TIRAP. Dots represent values of each individual of the investigated family. (E) The difference of gene expression in cells transfected with *TIRAP* or CTRL siRNA was calculated from mean values shown in panel D.

Figure 7. **TIRAP p.R81C enhances NF-kB activity and protects against stress-induced apoptosis.** 293T cells were transfected with TIRAP WT-GFP, TIRAP p.R81C-GFP or empty vector (EV)-GFP plasmids. Twenty-four hours post transfection, 293T cells were FACS purified for GFP-positive cells. (A) Heatmap showing hierarchical clustering of mRNA levels of six selected genes involved in NF-kB pathway, cell survival and proliferation within GFP-positive 293T cells. Bar chart showing the log2 fold difference of gene expression in transfected 293T cells (TIRAP p.R81C or WT versus EV) of a representative experiment. (B) FACS purified GFP-positive 293T were cultured in starvation medium for 48h, and cell viability was assessed by flow cytometry. Bar chart (mean ± SEM) show percentage of viable cells ($AnnexinV^-$ and Viability dye^-) of two independent experiments performed in replicates. One-way ANOVA with Bonferroni post hoc test was used, **P<0.05; **P<0.01, ***P<0.001*.

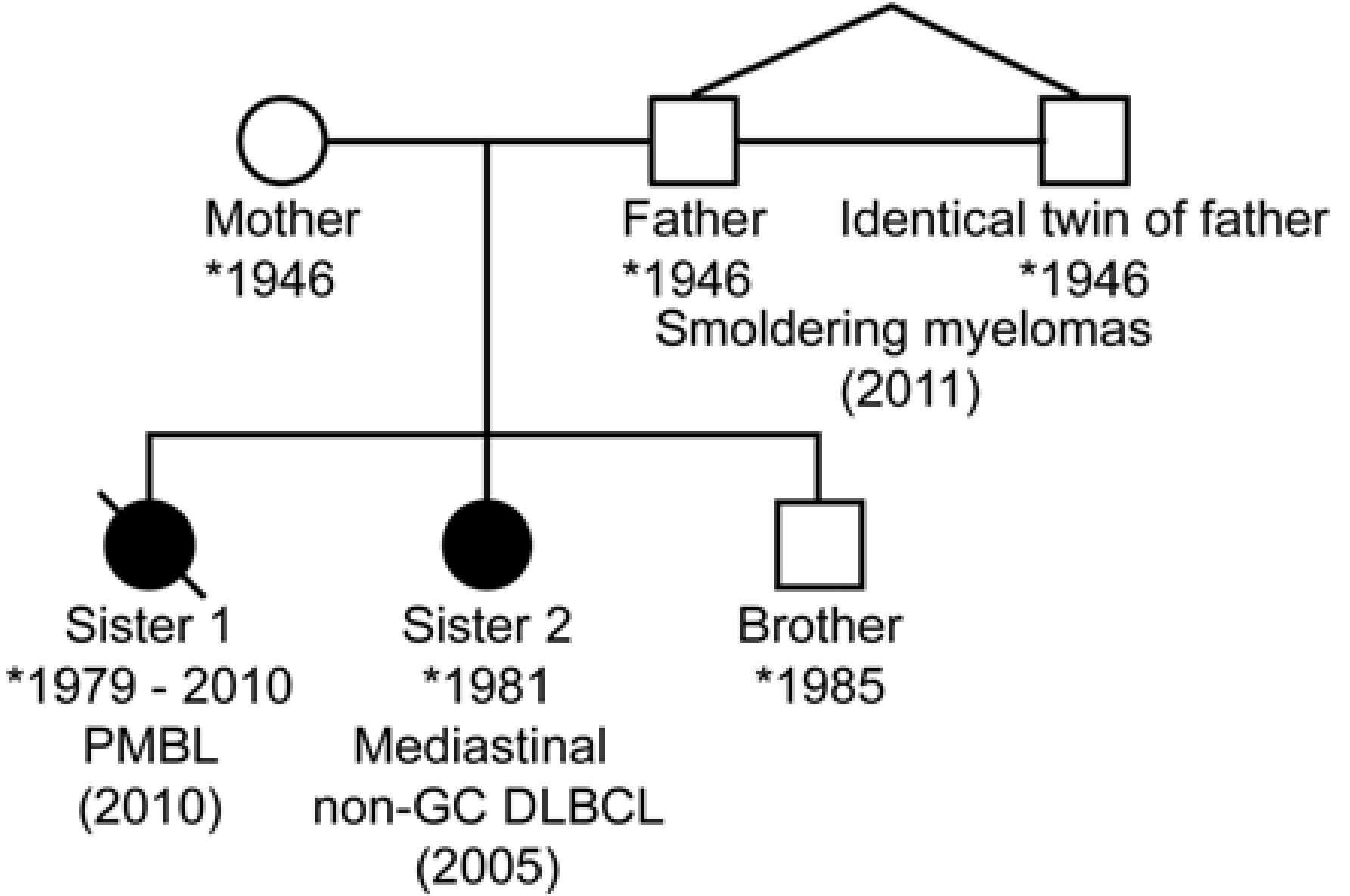
Mother
*1946
Father
*1946
Identical twin of father
*1946
Smoldering myelomas
(2011)
Sister 1
*1979 - 2010
PMBL
(2010)
Sister 2
*1981
Mediastinal
non-GC DLBCL
(2005)
Brother
*1985

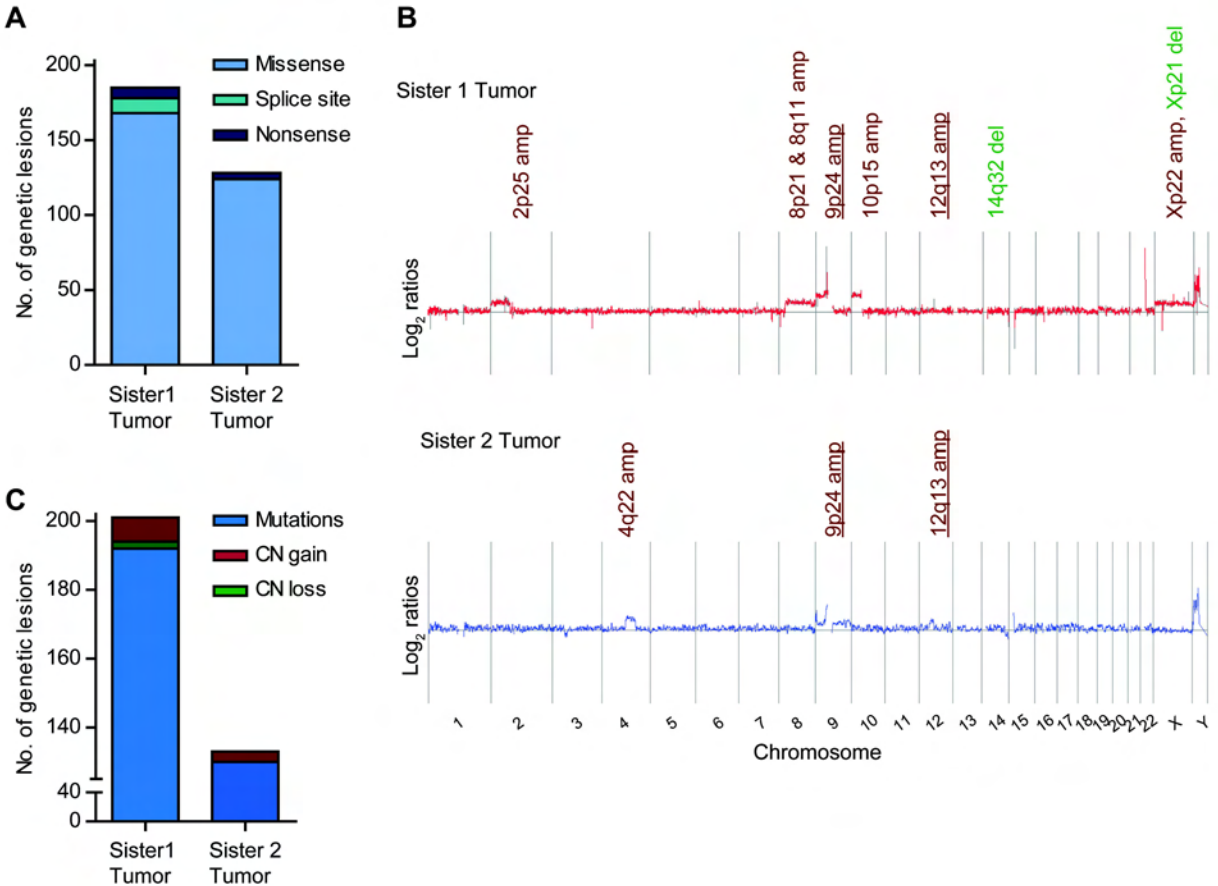
A
200
150
100
50
0
No. of genetic lesions
Missense
Splice site
Nonsense
Sister1 Tumor
Sister 2 Tumor
B
Sister 1 Tumor
2p25 amp
8p21 & 8q11 amp
9p24 amp
10p15 amp
12q13 amp
14q32 del
Xp22 amp, Xp21 del
Log2 ratios
Sister 2 Tumor
4q22 amp
9p24 amp
12q13 amp
Log2 ratios
1 2 3 4 5 6 7 8 9 10 11 12 13 14 15 16 17 18 19 20 21 22 X Y
Chromosome
C
200
180
160
140
40
0
No. of genetic lesions
Mutations
CN gain
CN loss
Sister1 Tumor
Sister 2 Tumor

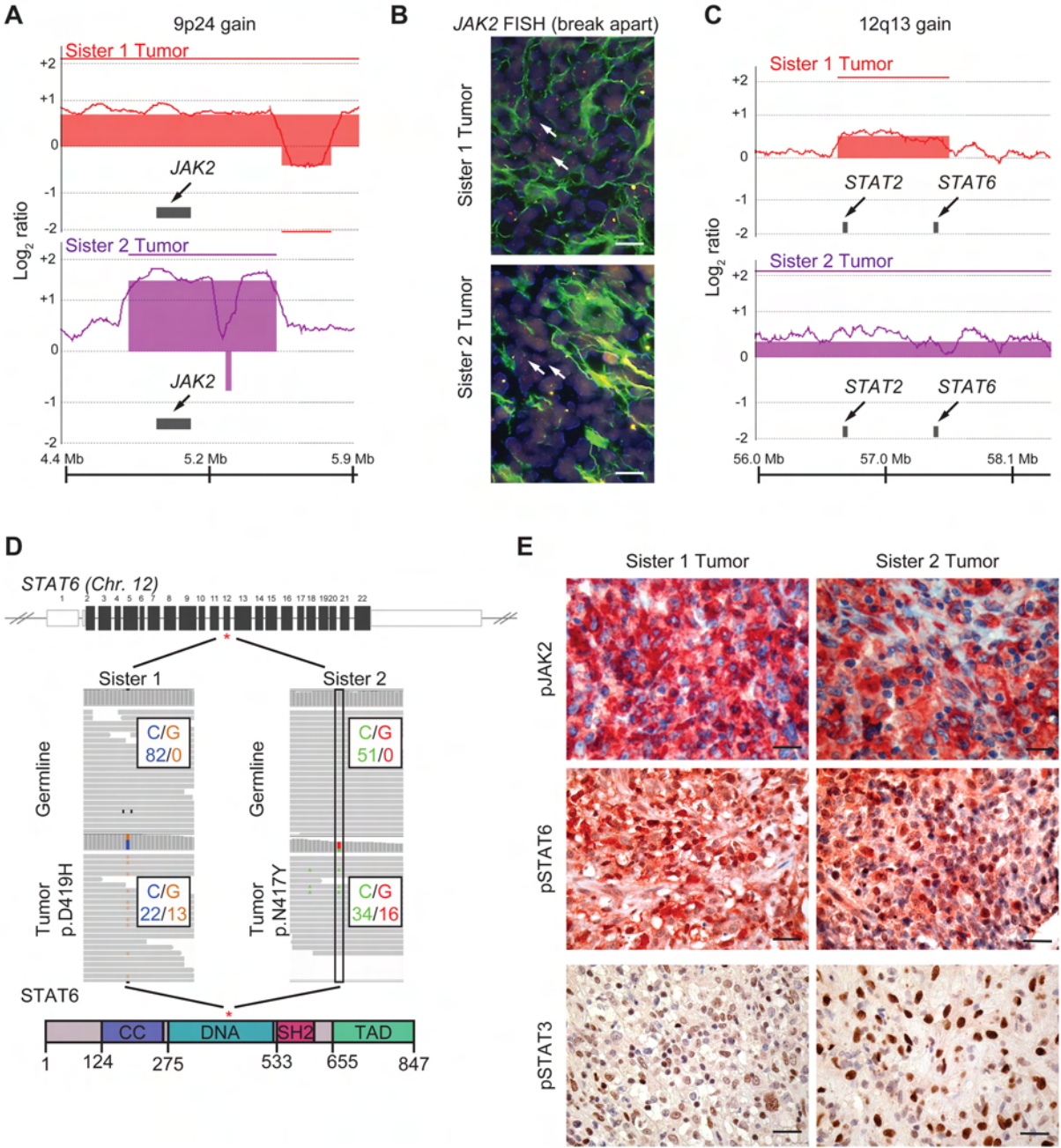
A
9p24 gain
Sister 1 Tumor
JAK2
Sister 2 Tumor
JAK2
Log2 ratio
4.4 Mb
5.2 Mb
5.9 Mb
B
JAK2 FISH (break apart)
Sister 1 Tumor
Sister 2 Tumor
C
12q13 gain
Sister 1 Tumor
STAT2
STAT6
Sister 2 Tumor
STAT2
STAT6
Log2 ratio
56.0 Mb
57.0 Mb
58.1 Mb
D
STAT6 (Chr. 12)
Sister 1
Sister 2
Germline
C/G
82/0
Germline
C/G
51/0
Tumor
p.D419H
C/G
22/13
Tumor
p.N417Y
C/G
34/16
STAT6
CC
DNA
SH2
TAD
1
124
275
533
655
847
E
Sister 1 Tumor
Sister 2 Tumor
pJAK2
pSTAT6
pSTAT3

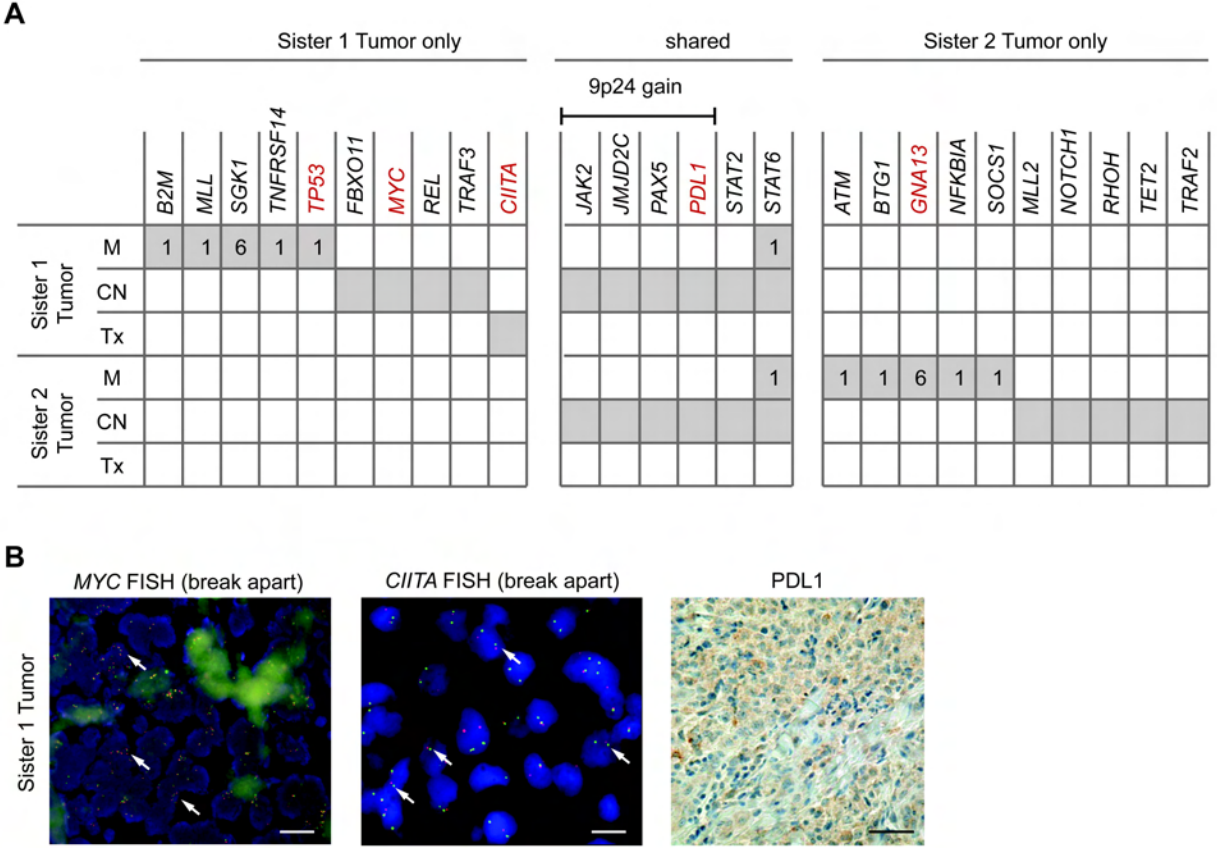
A
Sister 1 Tumor only
shared
Sister 2 Tumor only
9p24 gain
B2M
MLL
SGK1
TNFRSF14
TP53
FBXO11
MYC
REL
TRAF3
CIITA
JAK2
JMJD2C
PAX5
PDL1
STAT2
STAT6
ATM
BTG1
GNA13
NFKBIA
SOCS1
MLL2
NOTCH1
RHOH
TET2
TRAF2
Sister 1 Tumor
Sister 2 Tumor
M
CN
Tx
B
MYC FISH (break apart)
CIITA FISH (break apart)
PDL1
Sister 1 Tumor

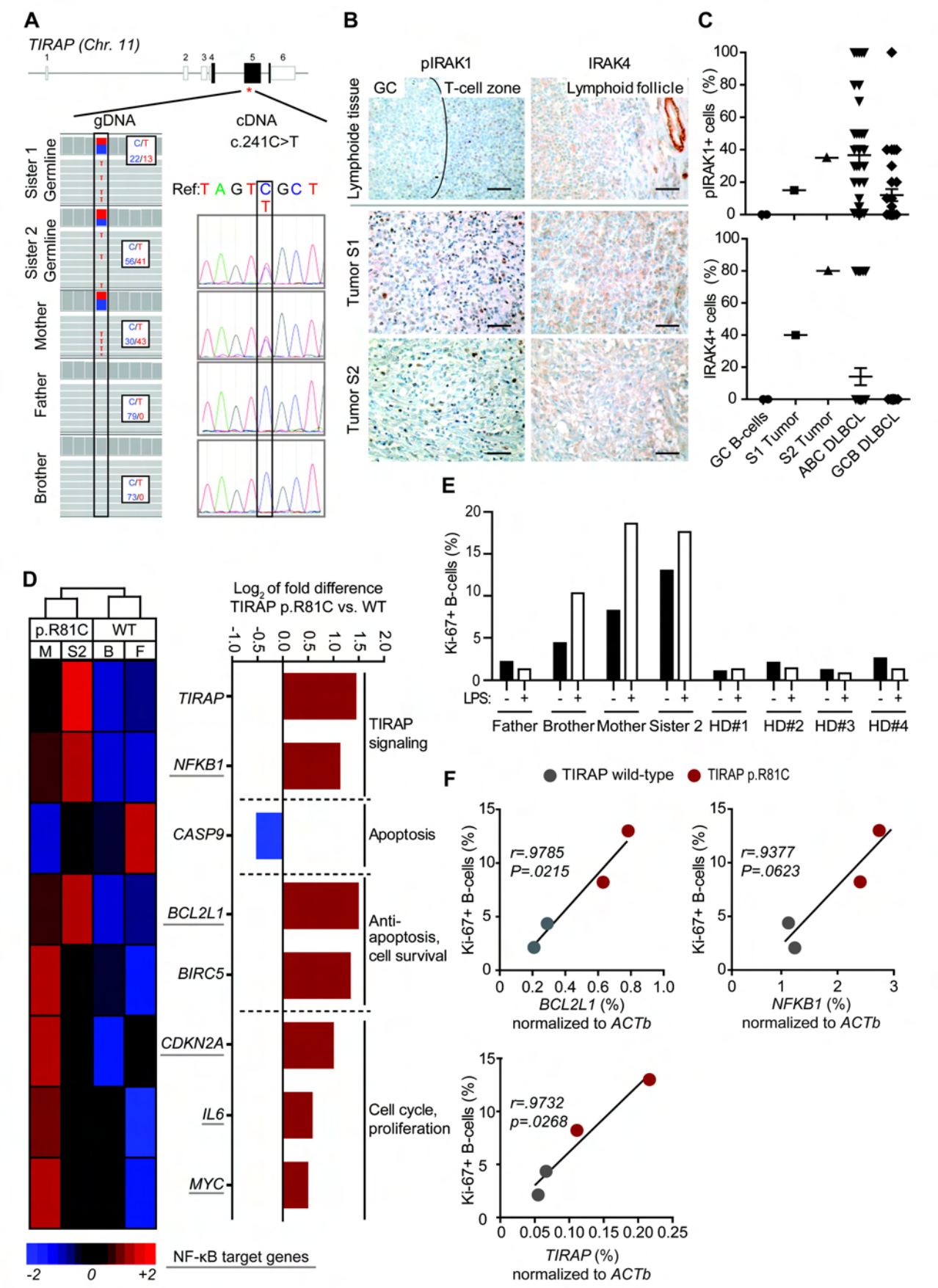
A
TIRAP (Chr. 11)
1
2
3 4
5
6
gDNA
cDNA
c.241C>T
Sister 1 Germline
Sister 2 Germline
Mother
Father
Brother
C/T 22/13
C/T 56/41
C/T 30/43
C/T 79/0
C/T 73/0
Ref:T A G T C G C T
T
B
pIRAK1
IRAK4
GC
T-cell zone
Lymphoid follicle
Lymphoide tissue
Tumor S1
Tumor S2
C
pIRAK1+ cells (%)
IRAK4+ cells (%)
GC B-cells
S1 Tumor
S2 Tumor
ABC DLBCL
GCB DLBCL
D
p.R81C
WT
M
S2
B
F
Log2 of fold difference
TIRAP p.R81C vs. WT
TIRAP
NFKB1
CASP9
BCL2L1
BIRC5
CDKN2A
IL6
MYC
TIRAP signaling
Apoptosis
Anti-apoptosis, cell survival
Cell cycle, proliferation
NF-κB target genes
E
Ki-67+ B-cells (%)
LPS:
Father
Brother
Mother
Sister 2
HD#1
HD#2
HD#3
HD#4
F
TIRAP wild-type
TIRAP p.R81C
r=.9785
P=.0215
BCL2L1 (%)
normalized to ACTb
r=.9377
P=.0623
NFKB1 (%)
normalized to ACTb
r=.9732
p=.0268
TIRAP (%)
normalized to ACTb

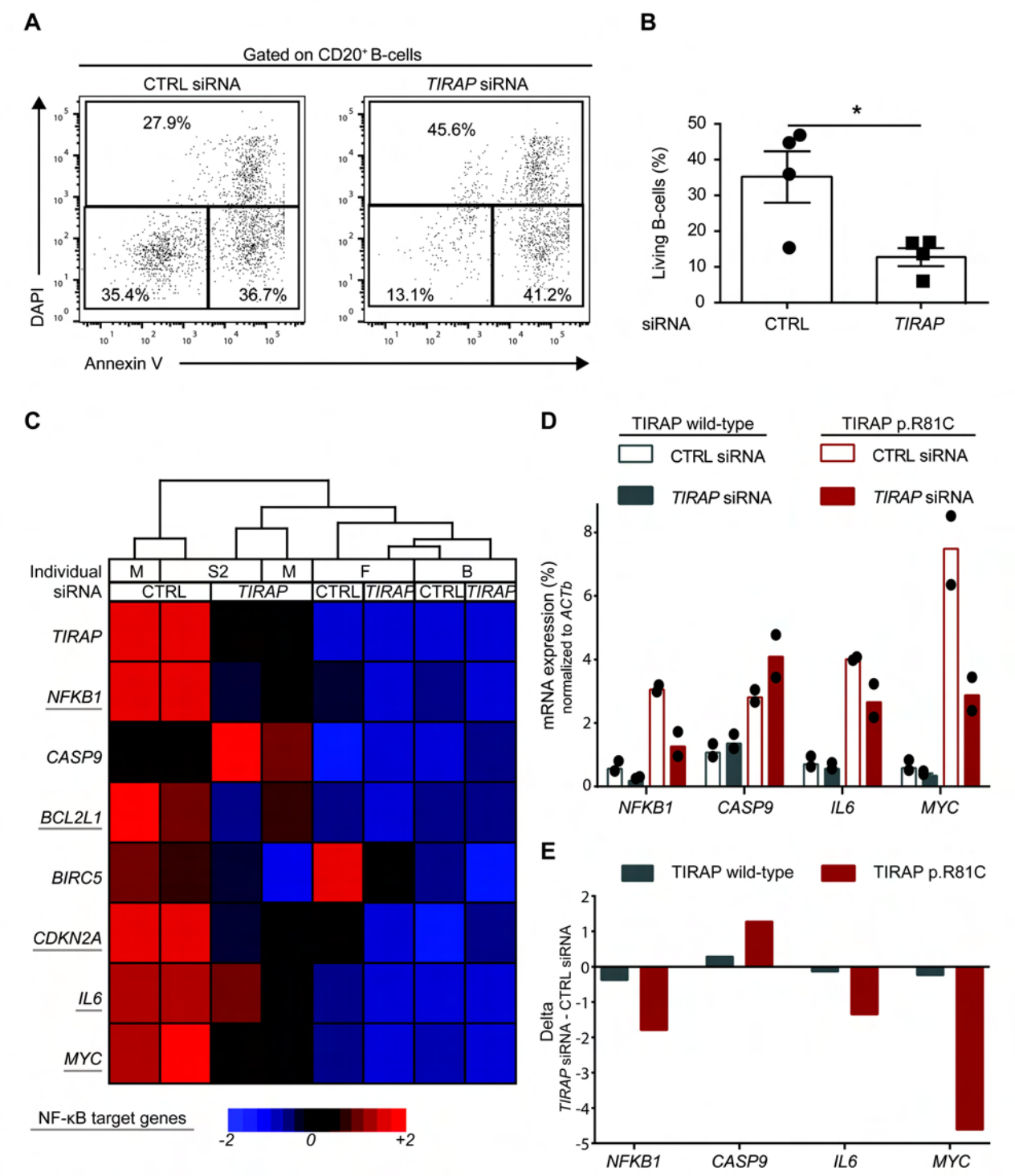
A
Gated on CD20+ B-cells
CTRL siRNA
TIRAP siRNA
27.9%
45.6%
35.4%
36.7%
13.1%
41.2%
DAPI
Annexin V
B
Living B-cells (%)
siRNA
CTRL
TIRAP
C
Individual
siRNA
M
S2
M
F
B
CTRL
TIRAP
TIRAP
NFKB1
CASP9
BCL2L1
BIRC5
CDKN2A
IL6
MYC
NF-κB target genes
-2
0
+2
D
TIRAP wild-type
TIRAP p.R81C
CTRL siRNA
TIRAP siRNA
mRNA expression (%)
normalized to ACTb
NFKB1
CASP9
IL6
MYC
E
TIRAP wild-type
TIRAP p.R81C
Delta
TIRAP siRNA - CTRL siRNA

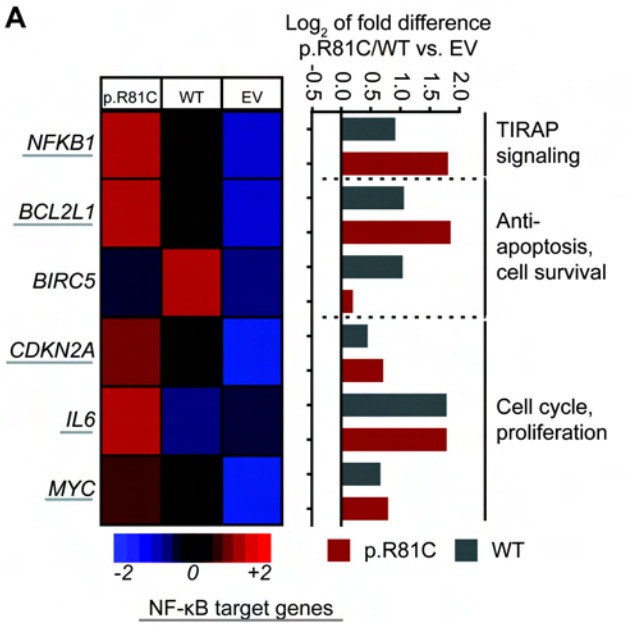
A
Log2 of fold difference
p.R81C/WT vs. EV
-0.5
0.0
0.5
1.0
1.5
2.0
p.R81C
WT
EV
NFKB1
BCL2L1
BIRC5
CDKN2A
IL6
MYC
TIRAP signaling
Anti-apoptosis, cell survival
Cell cycle, proliferation
p.R81C
WT
-2
0
+2
NF-κB target genes

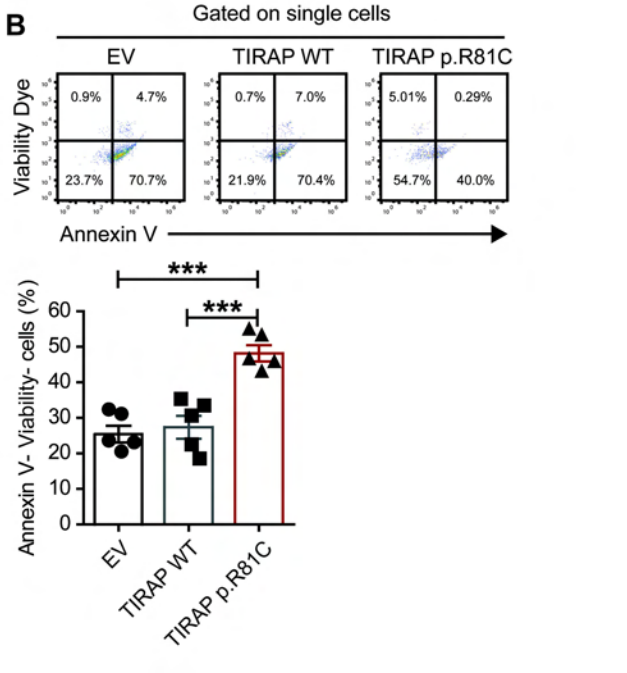
B
Gated on single cells
EV
TIRAP WT
TIRAP p.R81C
Viability Dye
0.9%
4.7%
23.7%
70.7%
0.7%
7.0%
21.9%
70.4%
5.01%
0.29%
54.7%
40.0%
Annexin V
***
***
Annexin V- Viability- cells (%)
60
50
40
30
20
10
0
EV
TIRAP WT
TIRAP p.R81C

Supplemental methods, tables and figures

TIRAP p.R81C is a novel lymphoma risk variant which enhances cell proliferation via NF-κB mediated signaling in B-cells

Regula Burkhard[1,2,3], Irene Keller[4], Miroslav Arambasic[1,2,3], Darius Juskevicius[5], Alexandar Tzankov[5], Pontus Lundberg[6], Rémy Bruggmann[4], Stephan Dirnhofer[5], Ramin Radpour[1,7,*] and Urban Novak[1,3,*,+]

[1] Department of Medical Oncology, Inselspital, Bern University Hospital, University of Bern, Bern, Switzerland.

[2] Division of Experimental Pathology, Institute of Pathology, University of Bern, Bern, Switzerland.

[3] Department for BioMedical Research (DBMR), University of Bern, Bern, Switzerland.

[4] Interfaculty Bioinformatics Unit, Department for BioMedical Research, and Swiss Institute of Bioinformatics, Bern, Switzerland.

[5] Institute of Pathology and Medical Genetics, University of Basel, Basel, Switzerland.

[6] Department of Biomedicine, Experimental Hematology, University Hospital Basel and University of Basel, Basel, Switzerland.

[7] Tumor Immunology, Department for BioMedical Research (DBMR), University of Bern, Bern, Switzerland.

[*] Co-senior authors

[+] to whom correspondence should be addressed

Supplemental methods

Analysis of somatic variants

Somatic variant calling and annotation. For the identification of somatic variants, the reads produced from germline and tumor samples of both sisters were mapped to the human reference genome (hg19) using bwa-mem v.0.7.5a, and PCR duplicates were identified with Picard-tools v.1.8.[1] Somatic variants were called using Strelka v.1.0.10 and SomaticSniper v.1.0.4.[2,3] Strelka was run using the configuration file for bwa provided with the tool, with default values for all options except isSkipDepthFilters which was set to 1 as recommended for WES data. Post-call filtering was applied as previously outlined.[2] In the SomaticSniper analysis, reads with a mapping quality of 0 were ignored and default values were used for all other options. Quality filtering was performed using our own script to retain only variants with at least three reads per allele and strand, and minimum base and mapping qualities of 30 for each allele. The variants detected by Strelka or SomaticSniper were combined and annotated using SnpEff v.3.2. in cancer mode.

Verification of somatic variants by Ion-Proton sequencing. To confirm somatic mutations identified by WES using the Illumina technology, we resequenced the tumor DNA from both sisters on an Ion-Proton sequencing system (Thermo Fisher Scientific). Library preparation was performed using the IonXpress Plus Fragment Library Kit (Thermo Fisher Scientific) according to the manufacturer's protocol. The resulting DNA libraries were pooled for the subsequent exome capturing which was performed with the Ion Target Exome Kit (Thermo Fisher Scientific). The enriched DNA libraries were then sequenced in a 500 flows run on a Proton instrument using V3 chemistry. The library preparation and sequencing was performed by Fasteris.

CLC Genomics Workbench software v.7.5.1 (Qiagen) was used to map the reads against the human reference genome (hg19) and perform a local realignment around indels. Variants were called using the Low Frequency Variant Detection tool, using a minimum coverage of 8, a minimum count of 2 and a minimum frequency of 20%.

Additionally, we compiled the total number of Ion Proton reads supporting each base at all positions where somatic variants had been detected based on the Illumina data. The goal of this step was to obtain tentative confirmation of variants at positions with low sequencing depth in the Ion Proton data. The base counts were compiled using the GATK's DepthOfCoverage tool based on alignment files produced with the Ion Reporter software by Fasteris.

Sanger Sequencing and validation of TIRAP p.R81C variant

TIRAP p.R81C variant and the expression of the mutated allele were assessed by sanger sequencing of cDNA isolated from peripheral blood mononuclear cells (PBMCs) of all family members. Primer sequences for validation are listed in Supplemental Table 6.

Isolation and in vitro culture of PBMCs

PBMCs from healthy donors or members of the studied family were isolated by density gradient centrifugation using Lymphoprep (Axis-Shield). Isolated cells were cultured in RPMI-1640, supplemented with 50 U/ml penicillin, 50µg/ml streptomycin (Sigma Aldrich) and 10% heat-inactivated human AB serum (Swiss Red Cross).

Proliferation assay and flow cytometry

PBMCs were cultured overnight in the presence or absence of 10ng/ml LPS (Thermo Fisher Scientific). Cells were stained with anti-CD20-PerCp-Cy5.5 (Biolegend). Intracellular staining with anit-Ki-67-PE (BD Bioscience) was performed using the Foxp3 staining Buffer set (eBioscience). After the final washing step, cells were resuspended in staining Buffer containing DAPI and incubated for 30 min. For live/dead cell discrimination, cells were washed in annexin V binding buffer (BD Bioscience) and stained with annexin V-FITC and DAPI (both Biolegend). Flow cytometry was performed using an LSR II (BD Biosciences) and analyzed with FlowJo software v.10 (TreeStar). Antibodies applied in this study are listed in Supplemental Table 4.

Small interfering RNA (siRNA)-mediated silencing of TIRAP gene

PBMCs were transfected with 50nM of commercially available human *TIRAP* (sc-42932) or scrambled siRNA (sc-37007, both Santa Cruz Biotechnology) using Lipofectamine LTX (Thermo Fisher Scientific) according to manufacturer's protocol and incubated for 16 hours in the presence or absence of 10ng/ml LPS. Thereafter, cells were subjected for the targeted gene expression or flow cytometry analysis.

Functional analysis of TIRAP p.R81C variant

Total of $8x10^5$ HEK 293T cells were seeded in 6-well plates and transiently transfected with 500ng of GFP-expressing constructs (pCCL.sin.PPT.hPGK.GFPWpre backbone) encoding TIRAP wild-type, TIRAP p.R81C or empty vector control. Twenty-four hours post transfection, cell viability and apoptosis were measured on GFP-positive cells. Therefore, cells were washed in Annexin V binding buffer (BD Bioscience) and stained with Viability Dye eFluor® 450 (eBioscience) and PE Annexin V (Immunotools). FACS-sorting was performed using FACS ARIA. Sorted GFP-positive cells were either used for RNA extraction (see below); or seeded at equal numbers in starvation medium (EBSS (Sigma) supplemented with 1% FCS) and incubated for 24 or 48 hours.

Targeted gene expression analysis

RNA from PBMCs of all family members or from transfected 293T cell was purified using RNeasy micro kit (Qiagen) and transcribed into cDNA using the High-Capacity cDNA Reverse Transcription kit (Thermo Fisher Scientific). In all PBMC samples, the total lymphocyte population accounted for 65% on average based on forward and site scatter in flow cytometry. qRT-PCR was assessed for a panel of selected genes (Supplemental Table 6) using FastStart Universal SYBR Probe Master (Roche). All reactions were performed on an ABI 7500 (Applied Biosystems) platform. Expression

levels of genes were normalized to *ACTb* mRNA and cells treated with *TIRAP* siRNA versus scrambled (CTRL) siRNA were compared using the $2^{-\Delta\Delta CT}$ method. Gene expression data was clustered using standard Euclidean's method based on the average linkage. Heatmaps were generated according to the standard normal distribution of the values (standardize makes mean of each column as zero, and scale it to standard deviation of 1 to making all the columns equal weight).

Array comparative genomic hybridization

For each hybridization, at least 300ng of genomic DNA from each sample and 500ng of commercial sex-matched 46 XX reference genomic DNA (Promega) were used. Reference and normal genomic DNA of sister 1 and 2 were digested by heat fragmentation at 95°C for 35 minutes. FFPE tissue-derived tumor samples needed no additional digestion. DNA fragmentation was evaluated by gel electrophoresis and image analysis with the ImageJ software (NIH). Subsequent sample labelling, hybridization and data analysis was performed as described.[4]

Immunohistochemistry

Immunohistochemistry was performed on serial tissue sections either manually overnight at 4°C or using an automated immunostainer Benchmark XT (Ventana/Roche) with a biotin-streptavidin peroxidase detection system according to the manufacturer's recommendations. For antibodies applied, see Supplemental Table 4. Cell of origin classification was done based on immunohistochemistry, as suggested by the current WHO classification[5], applying the so-called Tally algorithm, which has been proven to give the best concordance with microarray data.[6]

Fluorescent in situ Hybridization

Fluorescence *in situ* hybridization (FISH) was performed according to standard protocols on paraffin sections using bacterial artificial chromosome (BAC) clones for the 5' and 3' region of *JAK2* gene, BAC probes spanning the *TNFAIP3* gene in combination with a centromeric probe for chromosome 6 as described previously.[7,8] A Break Apart FISH assay designed to identify rearrangements of *CIITA* (16p13.13) was performed with a telomeric and centromeric BAC probe. Chromosomal translocations affecting *MYC* and *BCL2* were assessed by FISH using commercially available break apart probes from Vysis (Abott Molecular).[9] For further information see Supplemental Table 5.

Validation of GSTT1 loss

GSTT1 deletion status was examined by multiplex PCR in the tumor and matched normal DNA of both siblings as well as the germline DNA of healthy family members. Primer sequences for validation are listed in Supplemental Table 6.

Statistical analyses

Statistical analyses were performed using GraphPad Prism v.7 (GraphPad Software). Results are expressed as mean ± SEM if not stated otherwise. Comparisons were drawn using unpaired t-test,

Mann–Whitney U test or one-way Annova with Bonferroni post hoc test. The p values <0.05 were regarded as statistically significant with *$p<0.05$*, **$p<0.01$*, and ***$p<0.001$* (95% confidence interval).

Supplemental table 1. Characteristics of the lymphomas, treatment and outcome.

Patient	Age at diagnosis	Staging / involved sites	Diagnosis	Treatment	Outcome
Sister 1	30 years	IAE (mediastinal bulk)	PMBL	6x R-CHOP, 1x R, salvage with high-dose MTX & cytarabine and R-ICE	Died with primary progressive disease
Sister 2	25 years	II A / anterior mediastinum, supraclavicular region	Non-GC DLBCL NOS with features of PMBL	6x R-CHOP	Ongoing remission

Abbreviations: DLBCL, diffuse large B-cell lymphoma; GC, germinal center; NOS, not otherwise specified; r, rituximab; CHOP, cyclophosphamide, doxorubicin, vincristine, prednisone; ICE, ifosfamide, carboplatin, etoposide; MTX, methotrexate; PMBL, primary mediastinal B-cell lymphoma.

Supplemental table 2. The immunopathological features of the lymphomas.

	Sister 1	Sister 2
Diagnosis	PMBL	Non-GC DLBCL with features of PMBL
EBV	-	-
BCL2	+	-
BCL6	7-8%	1-2%
CD10	+	-
GCET1	+	-
LMO2	80%	20%
FOXP1	7-8%	-
MUM1p	40%	40%
CD20	+	+
CD23	+	-
CD30	+	+
Ki-67	65%	50%
pJAK2	>80%	>80%
pSTAT3	40%	60%
pSTAT6	30%	50%
TNFAIP3 FISH	2n	2n
BCL2 FISH	2n / no break	2n / no break
MYC FISH	5n	2n
CIITA FISH	Break apart	No break
JAK2 FISH	9p24 (gain)	9p24 (gain)

Abbreviations: DLBCL, diffuse large B-cell lymphoma; GC, germinal center; -, negative staining, +, positive staining.

Supplemental table 3. Exome data metrics.

Sample	Enrichment kit	Sequenced in (year)	Read pairs (mio)	Bases (GB)	mapped unique reads (#)	Mean cover-age ±100bp (fold)
Sister 1 Tumor	TrueSeq (15013230 Rev. A)	2012	32	6.39	13.5 mio 46.2%	20
Sister 1 Germline	TrueSeq (15013230 Rev. A)	2012	63	12.62	43.5 mio 70.6%	61
Sister 2 Tumor	TrueSeq (15013230 Rev. A)	2012	48	9.68	3.1 mio 6.9%	4
Sister 2 Germline	TrueSeq (15013230 Rev. A)	2012	55	11.01	39.6 mio 74.0%	55.9
Sister 2 Tumor	Nextera (15032301 Rev. A)	2013	96	26.2	19.8 mio 23.1%	12.1
Sister 2 Germline	Nextera (15032301 Rev. A)	2013	54	9.7	33.2 mio 75%	32.6
Mother Germline	TrueSeq (15013230 Rev. A)	2013	53	10.63	48.3 mio 95.3%	53.82
Father Germline	TrueSeq (15013230 Rev. A)	2013	52	10.42	48 mio 95.1%	56.41
Brother Germline	TrueSeq (15013230 Rev. A)	2014	45	8.9	29.1 mio 74 %	28.9

Supplemental table 4. Antibodies used for Flowcytometry (FC) and immunohistochemistry (IHC) on formalin-fixed paraffin-embedded tissue, antigen retrieval procedure and cut-off scores for IHC.

Antibody	Appli-cation	Clone	Conjugated to	Catalog #	Source	Cut-off score
BCL2	IHC	SP66	unconjugated	790-4604	Vetana/Roche	70%[10]
BCL6	IHC	GI191E/A8	unconjugated	760-4241	Vetana/Roche	30%[11]
CD10	IHC	SP67	unconjugated	790-4506	Vetana/Roche	20%[11]
CD20	IHC	L26	unconjugated	760-2531	Vetana/Roche	no cut-off
CD23	IHC	SP23	unconjugated	790-4408	Vetana/Roche	any expres-sion
CD30	IHC	Ber-H2	unconjugated	790-4858	Vetana/Roche	any expres-sion
FOXP1	IHC	SP133	unconjugated	760-4611	Vetana/Roche	50%[12]
pIRAK1	IHC	polyclonal	unconjugated	Ab63484	Abcam	15%
IRAK4	IHC	Y279	unconjugated	Ab32511	Abcam	any expres-sion
GCET	IHC	RAM341	unconjugated	Ab68889	Abcam	60%[11]
KI67	IHC	MIB-1	unconjugated	IR626	Dako	no cut-off
LMO2	IHC	1A9-1	unconjugated	790-4368	Vetana/Roche	30%[11]
MUM1p	IHC	MRQ-43	unconjugated	760-4529	Vetana/Roche	70%[11]
PDL1	IHC	E1L3N	unconjugated	13684	Cell signaling	any expres-sion
pJAK2	IHC	C80C3	unconjugated	3776	Cell signaling	>8%[9]
pSTAT3	IHC	D3A7	unconjugated	9145	Cell Signaling	17%[9]
pSTAT5	IHC	C11C5	unconjugated	9359	Cell signaling	16%[9]
pSTAT6	IHC	-	unconjugated	ab28829	Abcam	>5%
CD20	FC	2H7	PerCP/Cy5.5	302326	Biolegend	-
Ki-67	FC	B56	PE	556027	BD	-
AnnexinV	FC		FITC	556419	BD	-
DAPI	FC			422801	Biolegend	-
AnnexinV	FC		PE	31490014	Immunotools	
Live/Dead	FC		PacificBlue	65-0863-14	eBioscience	

Supplemental table 5. Probes for fluorescence *in situ* hybridization (FISH).

Locus	BAC clones	Reference
TNFAIP3	RP11-703G8, RP11-102P5	8
BCL2 Break apart	07J75-001 (Vysis, Abott)	9
cMYC Break apart	05J75-00, 05J91-001 (Vysis, Abott)	9
JAK2 Break apart	RP11-3H3, RP11-2302 and RP11-28A9, RP11-60G18	7
CIITA Break apart	RP11-109M19, RP11-66H6	13

Supplemental table 6. Used primers.

Primer Name	Sequence (5' to 3')
Primers for validation by Sanger sequencing	
GSTT1 Forward	TTCCTTACTGGTCCTCACATCT
GSTT1 Reverse	GCAGCATAAGCAGGACTTCAG
B-Globin Forward	CAACTTCATCCACGTTCACC
B-Globin Reverse	GAAGAGCCAAGGACAGTTAC
TIRAP Forward	GCTGAAGAAGCCCAAGAAGAG
TIRAP Reverse	GCTGCCTTCCAAGTAGGAGAC
Primers for quantitative PCR	
ACTB Forward	GCACCACACCTTCTACAATGAG
ACTB Reverse	GGTCTCAAACATGATCTGGGTC
BIRC5 Forward	CGCATCTCTACATTCAAGAACTG
BIRC5 Reverse	CCAAGTCTGGCTCGTTCTC
BCL2L1 Forward	AGGCGGATTTGAATCTCTTTCTC
BCL2L1 Reverse	AAACACCTGCTCACTCACTG
CDKN2A Forward	CACCAGAGGCAGTAACCA
CDKN2A Reverse	CTGATGATCTAAGTTTCCCGAG
CASP9 Forward	CAGATTTGGCTTACATCCTGAG
CASP9 Reverse	CCGCAACTTCTCACAGTC
IL6 Forward	GTGTGAAAGCAGCAAAGAGG
IL6 Reverse	GGCAAGTCTCCTCATTGAATCC
MYC Forward	TCCTCGGATTCTCTGCTCTC
MYC Reverse	CTTGTTCCTCCTCAGAGTCG
NFKB1 Forward	AAGCACGAATGACAGAGGC
NFKB1 Reverse	TTTCCCGATCTCCCAGCT
TIRAP Forward	GTCACTACGGCCTTACATAGGA
TIRAP Reverse	TCATGGAGCAGCCATCAG

Supplemental Table 7. Confirmed somatic mutations (Included in a separated Excel file).

Excel spreadsheet showing confirmed protein-altering somatic mutations identified in the lymphoma of sister 1 and 2.

Supplemental figure 1

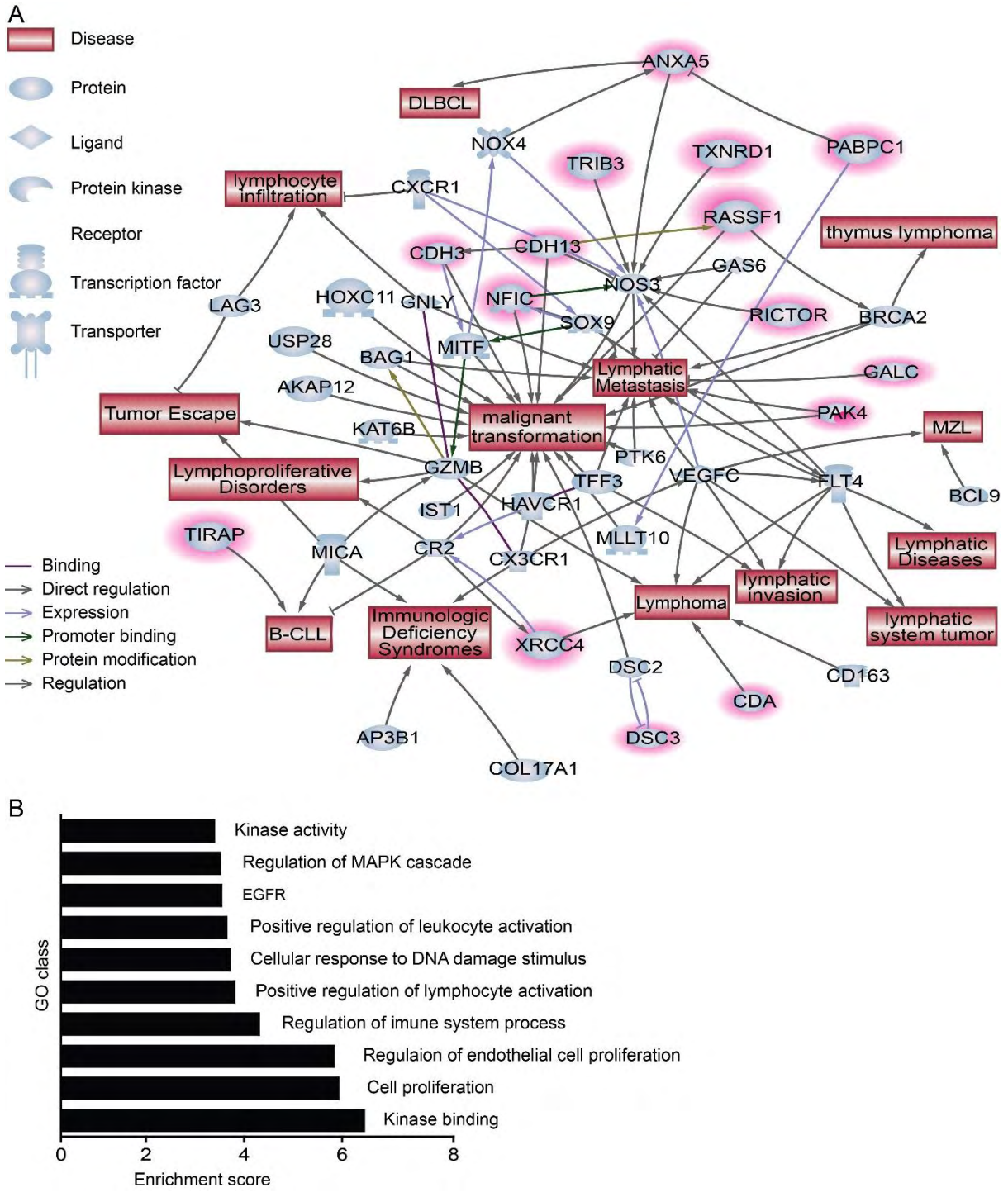

Supplemental figure 1. (A) Prediction of potential links between genes with germline variants and terms related to cancer and malignant lymphomas. Genes with variants predicted to be likely pathogenic by five different algorithms are highlighted in red. (B) Gene ontology enrichment analysis of the genes with deleterious variants. Enrichment score >3 are significant, $p<0.05$.

Supplemental figure 2

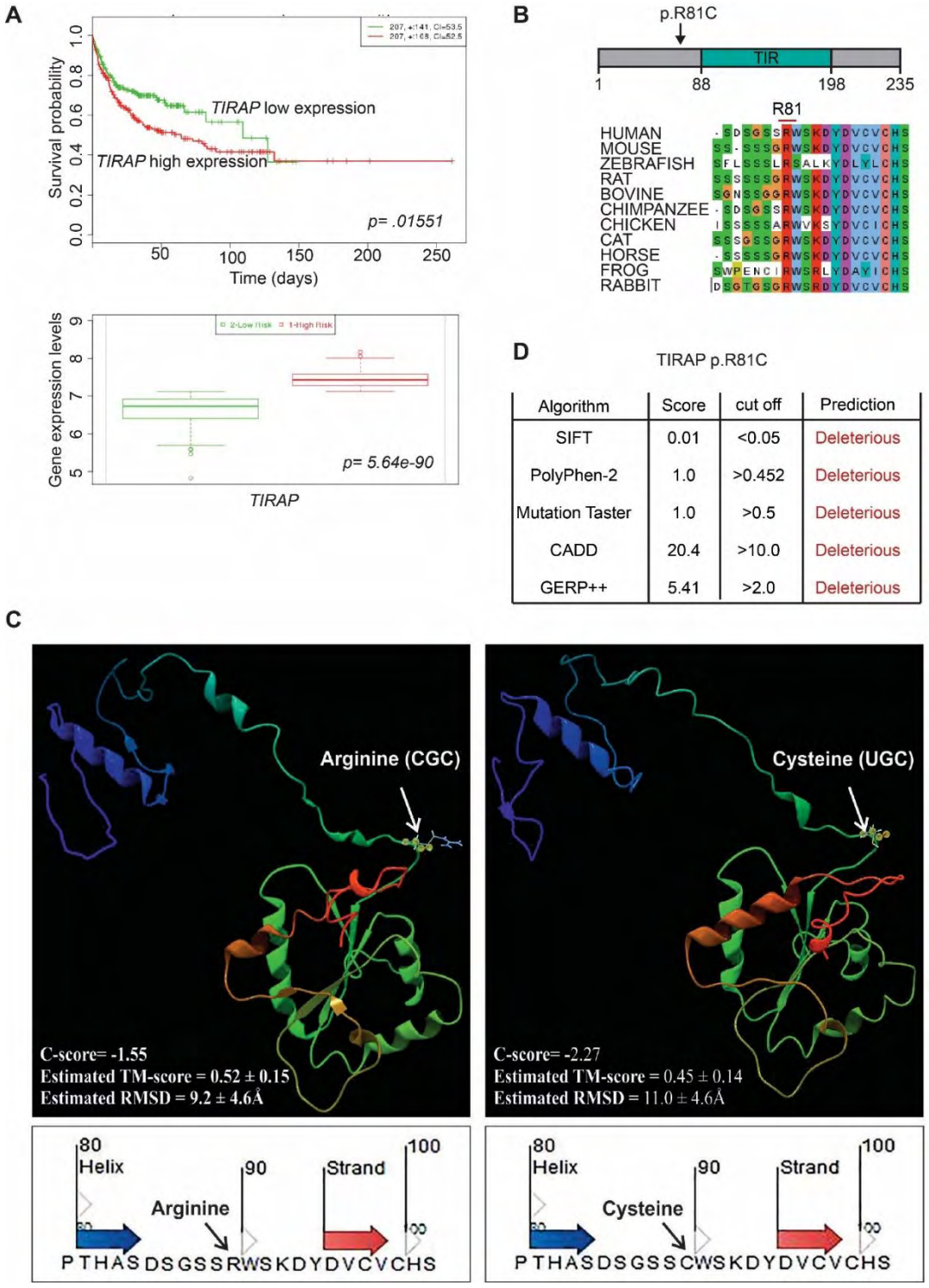

Supplemental figure 2. (A) Analysis of survival and *TIRAP* gene expression in patients with DLBCL. Kaplan-Meier survival curves (top) and box plots (bottom) showing the TIRAP mRNA expression (generated by the SurvExpress program from samples of the GSE10846 dataset). (B) Top: Schematic diagram of the TIRAP protein showing the TIR domain and the position of p.R81C missense mutation. Protein domain annotation according to Pfam. Below: TIRAP amino acid conservation among different species, R81 residue is marked in red. Sequence were aligned using ClustalW2. (C) 3D-structure prediction for TIRAP protein. I-TASSER server was used to generate a full-length model of TIRAP WT (left panel) and TIRAP p.R81C (right panel) by continuous frag-

ments from threading alignments and reassembling them using replica-exchanged Monte Carlo simulations. C-score is a confidence score for estimating the quality of predicted models based on the significance of threading template alignments and the convergence parameters of the structure assembly simulations. TM-score and RMSD are standards to measure the accuracy of structure modeling particularly when the native structure is not known. (D) The effect of the TIRAP p.R81C mutation was assessed in silico by SIFT, PolyPhen-2, MutationTaster, CADD and GERP++.

Supplemental figure 3

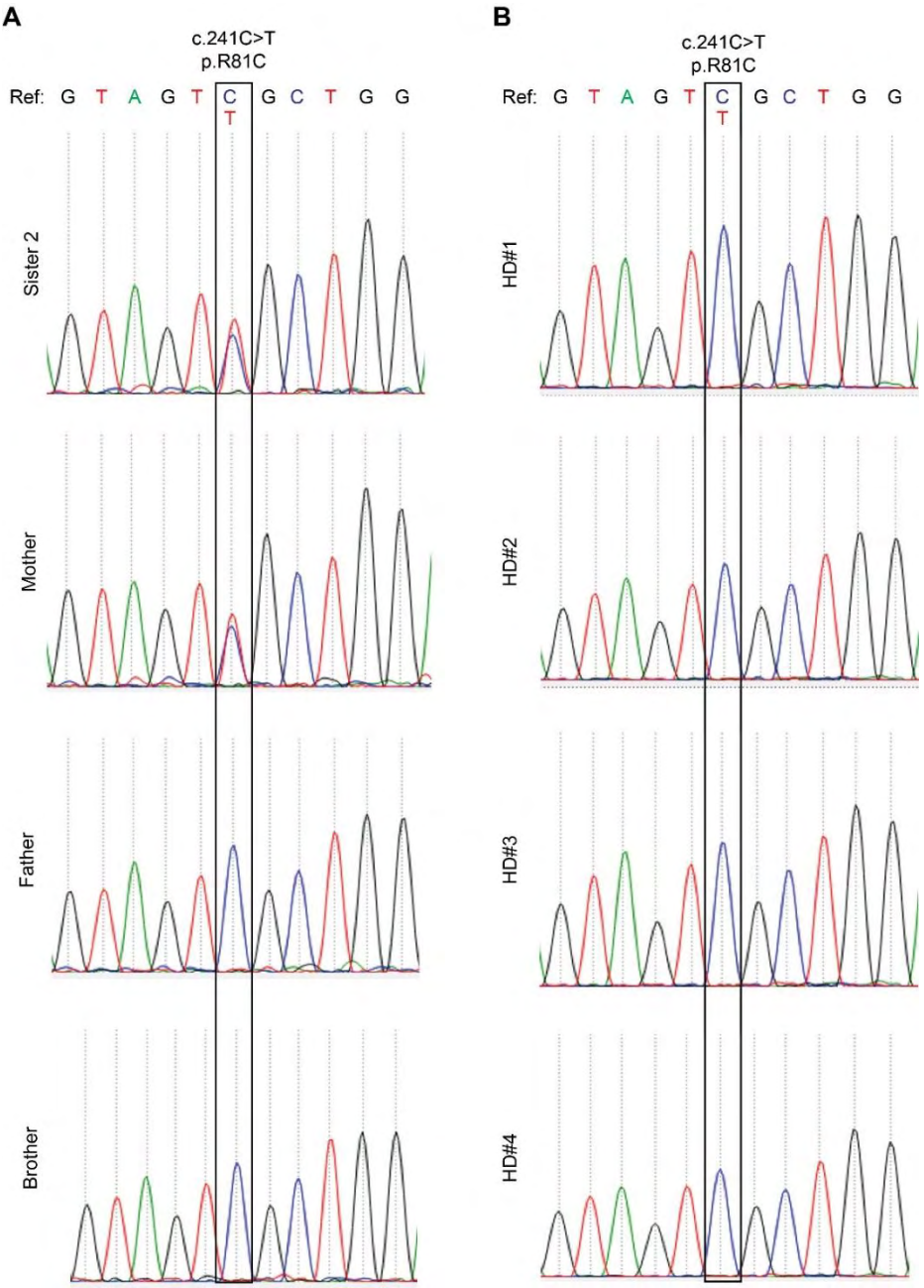

Supplemental figure 3. Analysis of *TIRAP* p.R81C mutation status by Sanger sequencing of (A) Sequencing result of isolated cDNA from PBMCs of all family members. (B) Genomic DNA isolated from PBMCs of age- and sex-matched healthy donors (HD).

Supplemental figure 4

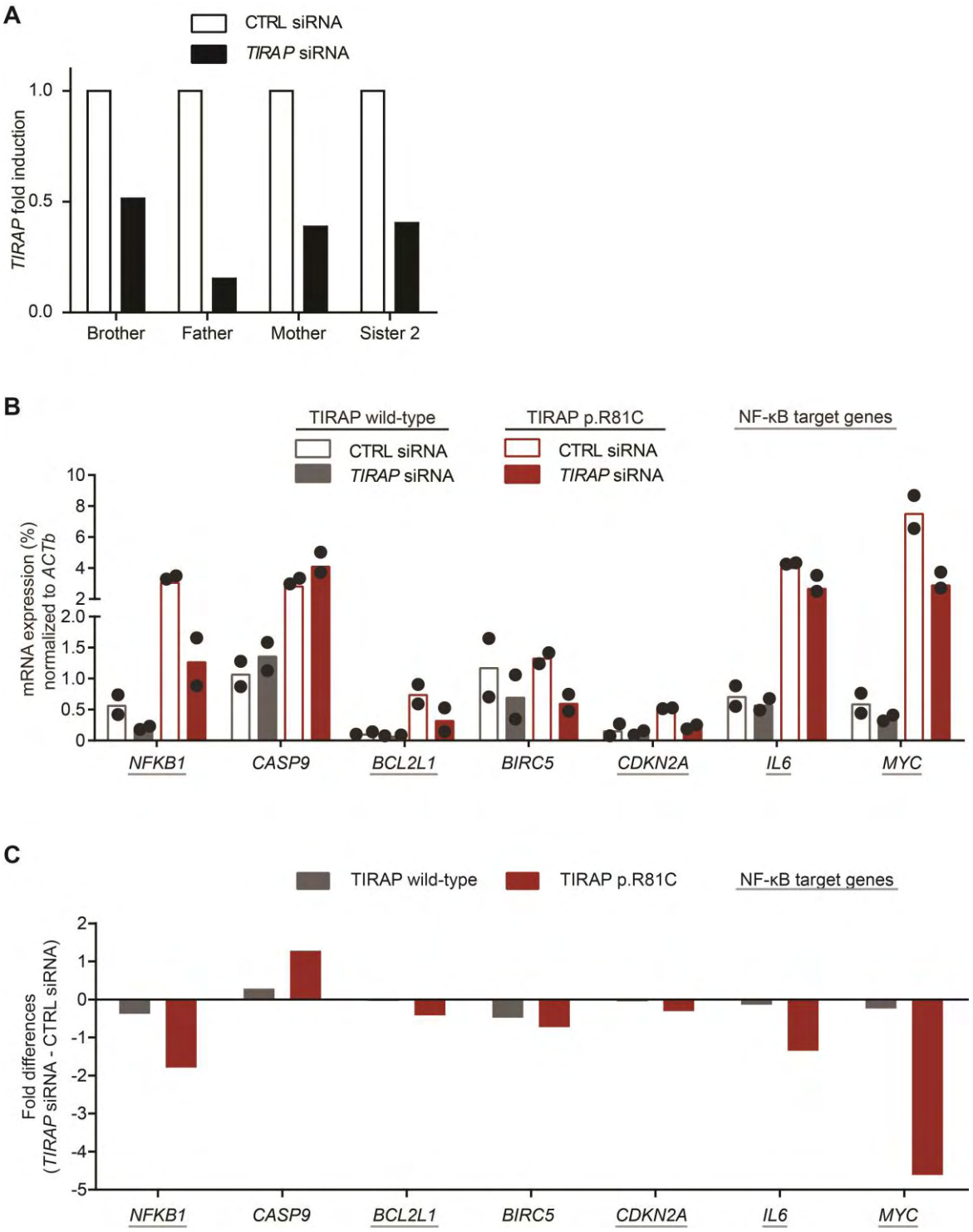

Supplemental figure 4. PBMCs were isolated from family members and transfected with control (CTRL) or *TIRAP*-directed siRNA. (A) Validation of *TIRAP* knockdown efficiency by qRT-PCR 24h post transfection. Values are shown as fold difference compared to cells transfected with CTRL-siRNA. (B) Bar chart showing the relative expression levels of genes involved in NF-κB pathway, cell survival and proliferation normalized to *ACTb* in PBMCs of family members with wild-type (brother and father) and p.R81C (sister 2 and mother) TIRAP. Dots represent values of each individual of the investigated family. (C) The difference of gene expression in cells transfected with *TIRAP* or CTRL siRNA was calculated from mean values shown in panel B.

Supplemental figure 5

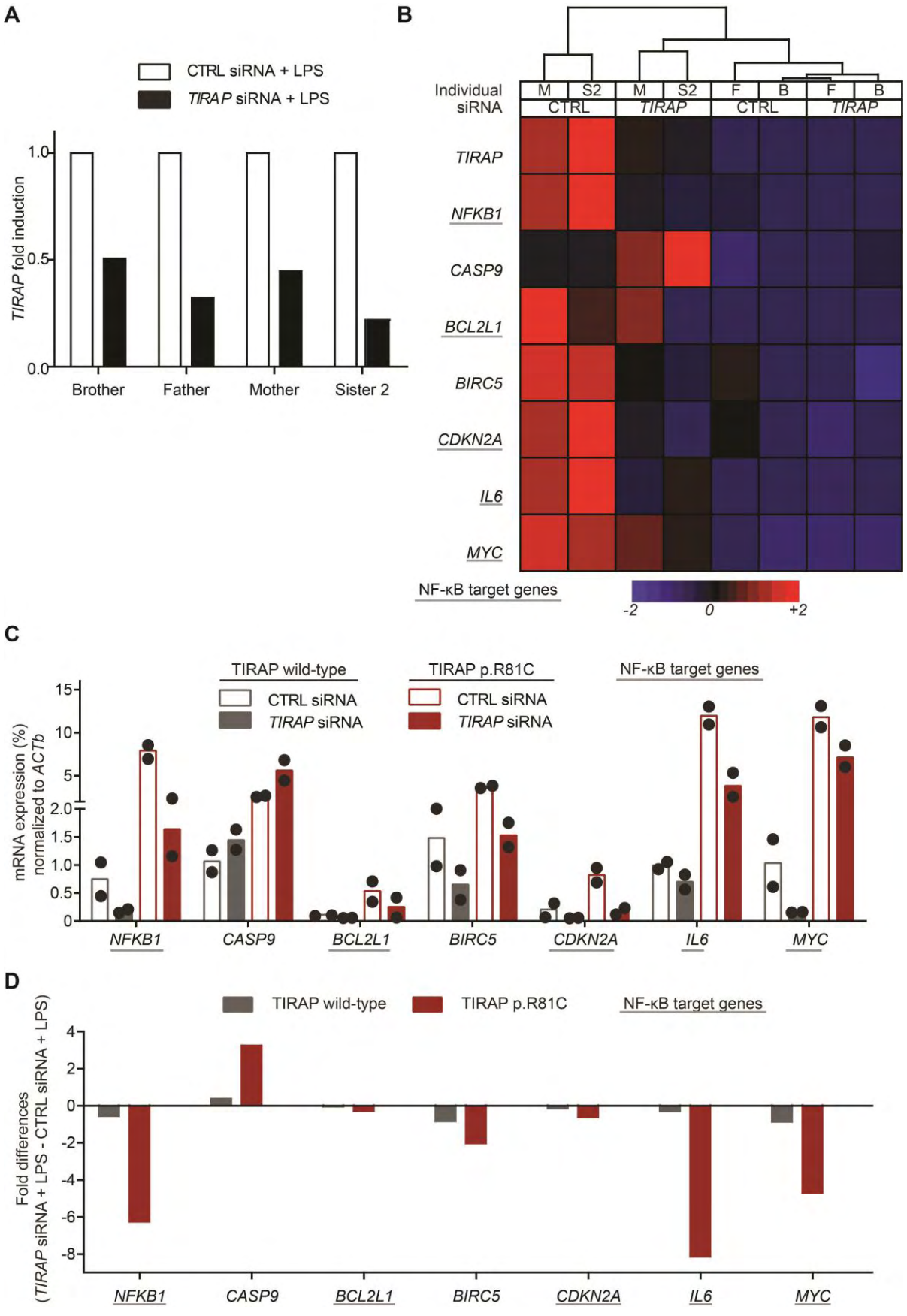

Supplemental figure 5. PBMCs were isolated from family members and transfected with control (CTRL) or *TIRAP*-directed siRNA and cultured in the presence of 10ng/ml LPS. (A) Validation of *TIRAP* knockdown efficiency by qRT-PCR 24h post transfection. Values are shown as fold difference compared to cells transfected with CTRL-siRNA. (B) Heatmap showing hierarchical clustering of eight selected genes involved in NF-κB signaling pathway, cell survival and proliferation in PBMCs of mother (M), sister 2 (S2), brother (B) and father (F) transfected with control (CTRL) or *TIRAP*-directed siRNA and treated with LPS. (C) Bar chart showing the relative expression levels normalized to *ACTb* in PBMCs of family members with wild-type (brother and father) and p.R81C (sister 2 and mother) TIRAP. Dots represent values of each individual of the investigated family. (D) The difference of gene expression in cells transfected with *TIRAP* or CTRL siRNA and treated with LPS was calculated from mean values shown in panel C.

Supplemental figure 6

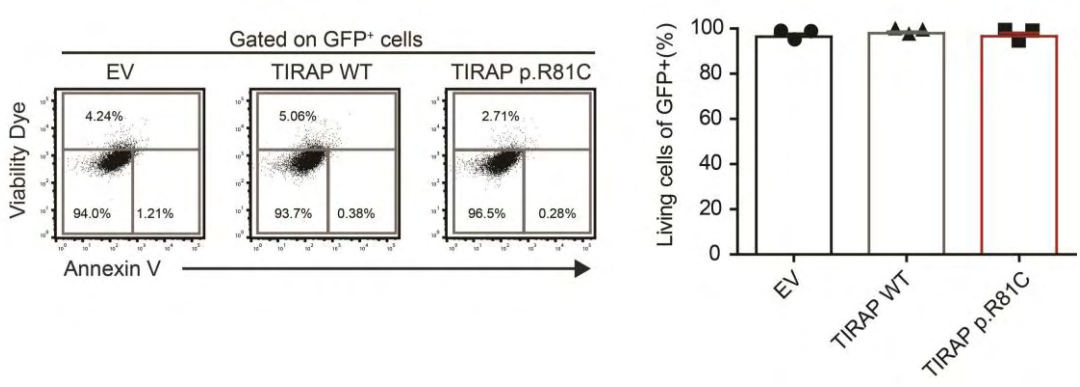

Supplemental figure 6. 293T cells were transiently transfected with TIRAP WT-GFP, TIRAP p.R81C-GFP expressing plasmids or empty vector (EV)-GFP plasmids. Cell viability on GFP-positive cells was assessed 24h post transfection by flow cytometry. Bar chart (mean ± SEM) show percentage of viable cells (AnnexinV- and Viability dye-) of GFP$^+$ cells of three independent experiments.

Supplemental figure 7

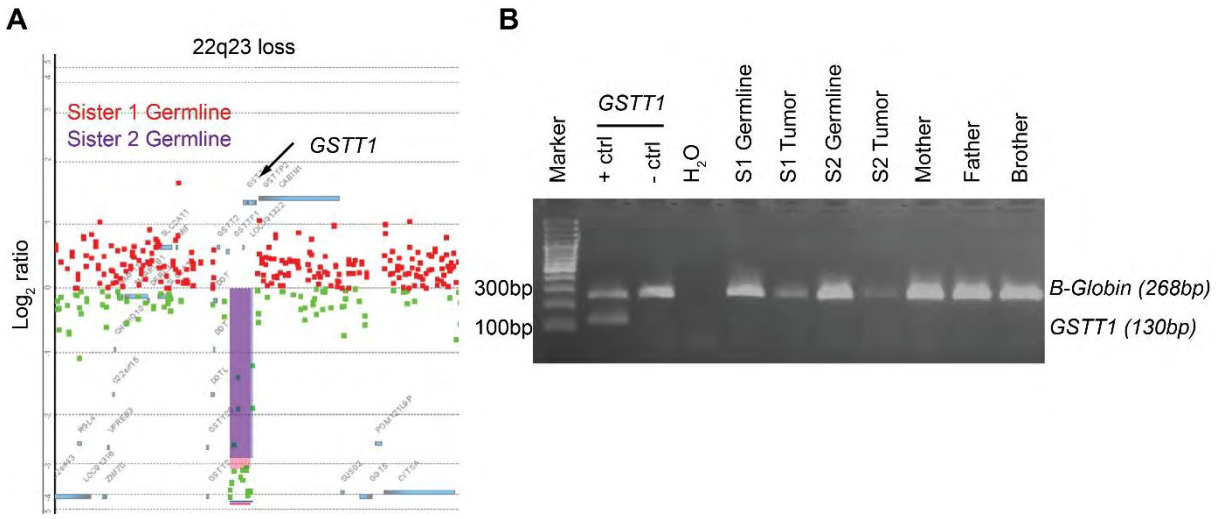

Supplemental figure 7. (A) aCGH probe view of the 22q loss in sister 1 (red) and 2 (purple). The *GSTT1* locus is indicated by an arrow. (B) *GSTT1* gene loss was analyzed in genomic DNA of all family members by a multiplex PCR using *B-globin* as an internal control. The resulting PCR products were analyzed on a 1.5% agarose gel. Amplification of *GSTT1* yields in a 130bp product. The fragment of 268bp corresponds to the *B-globin*. The absence of *GSTT1* (in the presence of a *B-globin* PCR product) indicates a *GSTT1* null genotype.

References

1. Li H. Aligning sequence reads, clone sequences and assembly contigs with BWA-MEM. arXiv:13033997 [Epub ahead of print].

2. Saunders CT, Wong WSW, Swamy S, Becq J, Murray LJ, Cheetham RK. Strelka: accurate somatic small-variant calling from sequenced tumor-normal sample pairs. Bioinforma Oxf Engl 2012;28(14):1811–1817.

3. Larson DE, Harris CC, Chen K, et al. SomaticSniper: identification of somatic point mutations in whole genome sequencing data. Bioinformatics 2012;28(3):311–317.

4. Juskevicius D, Ruiz C, Dirnhofer S, Tzankov A. Clinical, morphologic, phenotypic, and genetic evidence of cyclin D1-positive diffuse large B-cell lymphomas with CYCLIN D1 gene rearrangements. Am J Surg Pathol 2014;38(5):719–727.

5. Swerdlow SH, World Health Organization, International Agency for Research on Cancer, editors. WHO classification of tumours of haematopoietic and lymphoid tissues. Revised 4th edition. Lyon: International Agency for Research on Cancer; 2017.

6. Meyer PN, Fu K, Greiner TC, et al. Immunohistochemical methods for predicting cell of origin and survival in patients with diffuse large B-cell lymphoma treated with rituximab. J Clin Oncol Off J Am Soc Clin Oncol 2011;29(2):200–207.

7. Meier C, Hoeller S, Bourgau C, et al. Recurrent numerical aberrations of JAK2 and deregulation of the JAK2-STAT cascade in lymphomas. Mod Pathol Off J U S Can Acad Pathol Inc 2009;22(3):476–487.

8. Novak U, Rinaldi A, Kwee I, et al. The NF-{kappa}B negative regulator TNFAIP3 (A20) is inactivated by somatic mutations and genomic deletions in marginal zone lymphomas. Blood 2009;113(20):4918–4921.

9. Tzankov A, Xu-Monette ZY, Gerhard M, et al. Rearrangements of MYC gene facilitate risk stratification in diffuse large B-cell lymphoma patients treated with rituximab-CHOP. Mod Pathol Off J U S Can Acad Pathol Inc 2014;27(7):958–971.

10. Johnson NA, Slack GW, Savage KJ, et al. Concurrent expression of MYC and BCL2 in diffuse large B-cell lymphoma treated with rituximab plus cyclophosphamide, doxorubicin, vincristine, and prednisone. J Clin Oncol Off J Am Soc Clin Oncol 2012;30(28):3452–3459.

11. Visco C, Li Y, Xu-Monette ZY, et al. Comprehensive gene expression profiling and immunohistochemical studies support application of immunophenotypic algorithm for molecular subtype classification in diffuse large B-cell lymphoma: a report from the International DLBCL Rituximab-CHOP Consortium Program Study. Leukemia 2012;26(9):2103–2113.

12. Hoeller S, Schneider A, Haralambieva E, Dirnhofer S, Tzankov A. FOXP1 protein overexpression is associated with inferior outcome in nodal diffuse large B-cell lymphomas with non-germinal centre phenotype, independent of gains and structural aberrations at 3p14.1. Histopathology 2010;57(1):73–80.

13. Roberti A, Dobay MP, Bisig B, et al. Type II enteropathy-associated T-cell lymphoma features a unique genomic profile with highly recurrent SETD2 alterations. Nat Commun 2016;712602.